Research Square

Preprints are preliminary reports that have not undergone peer review.
They should not be considered conclusive, used to inform clinical practice,
or referenced by the media as validated information.

Gamma and theta band auditory steady-state responses in acute patients with schizophrenia and their association with antipsychotic treatment outcome

Marco De Pieri

marco.depieri@hcuge.ch

University hospital Geneva https://orcid.org/0000-0003-2795-1722

Vincent Rochas

Cyril Petignat

Dafni Apostolopoulou

Michel Godel

Giorgio Di Lorenzo

Tor Vergata University of Rome https://orcid.org/0000-0002-0576-4064

Matthias Kirschner

University of Geneva

Stefan Kaiser

Article

Keywords:

Posted Date: November 13th, 2026

DOI: https://doi.org/10.21203/rs.3.rs-11155689/v1

License: This work is licensed under a Creative Commons Attribution 4.0 International License.
Read Full License

Additional Declarations: Yes Stefan Kaiser received advisory board honoraria from Boehringer and Exeltis as well as royalties for cognitive test and training softwares from Schuhfried. Matthias Kirschner received advisory board honoraria from Otsuka. The other authors declare no competing interest.

Gamma and theta band auditory steady-state responses in acute patients with schizophrenia and their association with antipsychotic treatment outcome

[1,2]Marco De Pieri*, [3]Vincent Rochas, [4]Cyril Petignat, [1]Dafni Apostolopoulou, [1]Michel Godel, [5,6]Giorgio Di Lorenzo, [1,4]Matthias Kirschner, [1,2,4]Stefan Kaiser

[1]Division of Adult Psychiatry, Department of Psychiatry, University Hospitals of Geneva
[2]Synapsy Center for Neuroscience and Mental Health Research, University of Geneva, Geneva Switzerland
[3]M/EEG & Neuromod platform, Fondation Campus Biotech Geneva, Switzerland
[4]Faculty of Medicine, University of Geneva, Geneva, Switzerland
[5]Department of Systems Medicine, Tor Vergata University of Rome, Rome Italy
[6]IRCCS Fondazione Santa Lucia, Rome, Italy

**Corresponding author at: Division of Adult Psychiatry, Department of Psychiatry, Geneva University Hospitals, 2, Chemin du Petit-Bel-Air, CH-1226 Thonex, Switzerland; Tel: +41-(0)-22 3055104; Fax: +4179 3054689.*
E-mail address: marco.depieri@hug.ch

ABSTRACT

Few schizophrenia EEG studies were realized during acute psychotic episodes, which represent a favorable vantage point to assess pathophysiology and to establish predictive biomarkers of response to antipsychotic medications.

The EEG 40 Hz auditory steady state response (ASSR) reflects the GABA-glutamate signaling and the excitation/inhibition imbalance and is impaired in schizophrenia.

High-density EEG was recorded in acute inpatients with schizophrenia (N=91) and healthy controls (N=45) to assess the ASSR metrics event related spectral perturbation (ERSP) and intertrial phase coherence (ITC), in both gamma (38-42 Hz) and theta (4-8 Hz) bands. Furthermore, we investigated the relationship of these parameters with response to antipsychotics and with positive, negative, disorganized, excited and depressive symptoms.

No ERSP and ITC differences emerged in gamma band between patients and controls. Patients showed reduced theta ITC in both the early (0-0.25s post-stimulus; d=-0.97; p=<.001) and the late (0.25-1.25s post-stimulus; p=0.024, d=-0.62) time windows compared to controls, and a similar reduction in ERSP (early: d=-0.88; P=<.001; late: d=-0.64; p=0.013). Responders to treatment showed reduced gamma ITC (early: d=-0.64, P=0.015; late: d=-0.62, p=0.025) and late ERSP (d=-0.57, p=0.025) compared to non-responders. Non-responders showed increased gamma ITC (early: d=0.65, p=0.002; late: d=0.61, p=0.010) and ERSP (early: d=0.57, p=0.024; late: d=0.67, p=0.005) compared to controls.

In conclusion, patients with schizophrenia having an acute psychotic episode display unexpected ASSR responses, with reduced theta ITC and ERSP, and no reduction in gamma activity. An increased gamma band activity characterizes the neurobiology of non-responders to antipsychotics, representing a candidate biomarker for treatment outcome stratification.

INTRODUCTION

In recent years, EEG research on schizophrenia has been conducted almost exclusively on stabilized outpatients, with acute inpatients left unstudied; however, studying brain dynamics during an acute psychotic episode could bring fundamental pieces of knowledge towards the understanding of schizophrenia pathophysiology.
Perhaps more importantly, recording brain activity in this setting could lead to the discovery of EEG biomarkers of response to antipsychotic medications, if an initial clinical and instrumental assessment is combined with a longitudinal evaluation. Such outcome would be of the outmost relevance: while antipsychotic medications represent the mainstay in the treatment of schizophrenia, their efficacy is often unsatisfactory, with response rates of 45-70% (1), and discontinuation rates of 32-74% (2). Moreover, interindividual variability in response to antipsychotics is large and unpredictable, giving rise to the practice of prescription by trial and error, requiring multiple attempts with different molecules, dose adjustments and drug combinations. Predictors of response remain elusive, with no candidate biomarker for antipsychotics selection having reached the clinical practice (3, 4) — a development that would be essential for delivering timely and effective treatments (5, 6).
EEG was already used to individuate neural signature of response to antipsychotic medications, however studies had a limited reach, due to small sample size and resting state only design (7).

One of the main hypothesis on the origin of schizophrenia posits that an altered interplay between pyramidal neurons and parvalbumin containing (PV) GABAergic interneurons, related to the hypoactivity of the N-methyl-D-aspartate (NMDA) glutamate receptors, would lead to the cortical excitation/inhibition (E/I) imbalance at core of schizophrenia pathophysiology (8, 9).
EEG gamma frequencies (i.e. brain oscillations in the 30–100 Hz frequency range) are considered an expression of that interplay, as they are generated through feedback inhibition on pyramidal neurons by parvalbumin containing (PV) interneurons (10, 11); the 25 ms decay rate of this inhibition particularly contributes to the generation of the 40 Hz signal (12).
Classically, both resting state and task related gamma band abnormalities were deemed important for schizophrenia; however, while the literature focusing on the resting state produced mixed, contradictory evidence (13), the results on task-related activity were more consistent, in particular concerning the auditory steady state response (ASSR; i.e. the oscillatory responses entrained to the frequency and phase of temporally modulated stimuli (14-16).
ASSR analysis comprises power (event related spectral perturbation, ERSP), and phase

(intertrial phase coherence, ITC) measures, in two time windows: an early phase reflecting event-related potential processes, and late latency sustained responses reflecting rhythmic activity (17).

Kwon et al first investigated 40-Hz ASSRs in patients with schizophrenia, demonstrating both a reduced power and a phase delay at the 40-Hz stimulation (18). After 27 years of research on the topic, ~50 studies have investigated 40 Hz ASSR in patients with schizophrenia using M/EEG, and the large majority found a reduction of both ITC and ERSP with medium-to-large effect size. Few of these also investigated the association of ASSR parameters with positive and negative symptoms of schizophrenia, with unconclusive results (14-16).

While E/I imbalance and glutamatergic dysfunction represent solid neurobiological mechanisms of schizophrenia, likely involved across phase and stages of the disorder (6, 19, 20), it is possible that the specific balance in E/I shifts during acute psychotic episodes, and that level of NMDA hypoactivity oscillates, leading to ASSR patterns different from what typically observed in stabilized patients.

The analysis of the ASSR classically only involved the gamma band; however, time frequency representations (TFR) from previous ASSR studies showed the induction of a large theta activity in healthy controls, not noticeable in patients (21-23). This activity seems relevant because increased resting-state theta activity is a main signature of schizophrenia (24-26), and related to disinhibition (27), and cognitive impairment (28, 29). This evidence sparked the curiosity to assess theta activity beyond the resting state, in a consolidated task-related context such as the ASSR.

In the present study we recruited inpatients with schizophrenia at the admission to the hospital and healthy controls, aimed to investigate relevant brain dynamics and clinical-neurophysiological correlations during an acute psychotic decompensation.

The primary objective of the study was to assess ASSR dynamics in acute patients with schizophrenia, by comparing them with healthy controls. We expected to find an impairment of both gamma-band ERSP and ITC, similarly to well replicated findings in stabilized outpatients, however with a larger effect size. In fact, we believed that E/I imbalance and NMDA hypofunction not only constitute the fundamental pathophysiological mechanisms of schizophrenia, operating in all phases and stages of the disease, but also that their exacerbation drives acute decompensations. Following the same logic, we expected that the reduction in ERSP and ITC would also correlate with positive and negative symptoms severity.

The secondary objective of the study was to assess the role of the ASSR as a predictor of the response to antipsychotics medications, that we expected to be related to lower ASSR

power (ERSP) and phase synchronization (ITC). Assuming that antipsychotics' mechanism of action consists of restoring the E/I imbalance, we anticipated that the larger the gamma impairment related to it, the more room for antipsychotics to exert a significant effect.

The analysis we conducted on theta band should be regarded as exploratory, given the lack of previous formal analysis during the ASSR tasks; nevertheless we formulated the hypothesis that the same theta band reduction in patients compared to controls observed in the images of previous studies exists also during the acute psychotic episode and is further exacerbated.

METHODS

Full details on recruitment, clinical assessment, EEG preprocessing and analysis are provided in **Supplementary methods**.

We recruited adult inpatients with schizophrenia during an acute psychotic episode and age-sex matched healthy controls. **Table S1** shows the criteria for participating in the study. Patients received a monotherapy or a combined therapy with a first- or second-generation antipsychotic medication. Patients were assessed upon admission and invited for a follow-up after six weeks, aimed to determine the efficacy of the antipsychotic treatment.

We evaluated the correlation between ASSR parameters and symptoms rating scales at the baseline assessment, including PANSS total score and subscales for positive, negative, disorganized, excited and depressed symptom dimensions (30).

Response to the antipsychotic treatment was defined as a ≥50% reduction in PANSS total score (31), and also the percentage change in PANSS total score between the two time points was considered as an outcome (32). Patients not accepting the follow-up evaluation were not included for the primary outcome on response to antipsychotic medications, and the attrition bias was analyzed.

The ASSR task was administrated using E-prime software v3.0, and it consisted of a 1000 Hz pure tone sound modulated in amplitude from minus infinite to 0 dB with a 40 Hz sinusoidal envelope, and flat sounds consisted of a 1000 Hz pure tone. Intertrial interval lengths were randomly picked between 0.5 and 2 sec and stimulus duration was 1.5s.

EEG was recorded with a 128-channel ANT Neuro EEGO MyLab system during a 40-Hz ASSR paradigm. We applied an automated preprocessing, involving band-pass (1-60 Hz) and notch (50Hz) filtering, bad channel removal and interpolation, line noise removal, denoising with the GEDAI toolbox (Generalized Eigenvalue De-Artifacting Instrument), artifact removal via ICA, bad epochs rejection.

All EEG analyses were performed in MNE-Python v1.7 on epoched data, limited to a region of interest (ROI) comprising 26 fronto-central electrodes. TFR were computed using the

Morlet transform, with 40-Hz Event-Related Spectral Perturbation (ERSP) and Inter-Trial Phase Coherence (ITPC) extracted for early (0-0.25s) and late (0.25-1.25s) windows; ERSP analysis involved a baseline correction relative to the -0.5 to -0.1s period before each epoch, and values were expressed in Decibel. EEG frequency bands selected for the analysis were 38-42 Hz (gamma band), and 4-8 Hz (theta band).

A temporal specificity analysis was conducted on the theta onset, including a wavelength control for the post-onset theta decay and the assessment of causal vs non causal theta envelopes, aimed at evaluating potential artifacts provoked by filtering and epoching procedures. Group differences (Patients vs. Controls; responders vs. non-responders; responders vs controls, non-responders vs controls) and the correlation between ASSR parameters and symptoms rating scales were assessed using non-parametric cluster-based permutation tests (10,000 permutations). False discovery rate (FDR) correction for multiple comparisons (for each frequency band, across ERSP and ITC in the early and late windows, 4 tests per family) and sensitivity analysis was realized for all the FDR significant outcomes. Because the reduction in 40 Hz ITC and ERSP is well quantified in previous ASSR literature (15), we complemented conventional significance testing of the gamma-band contrasts with equivalence testing against the effect size reported meta-analytically (33).

The study was approved by the Ethics Committee of the Geneva Canton (ID 2023–0535) and informed consent was obtained from all participants.

RESULTS

Clinical, socio-demographic and treatment characteristics

Table 1 shows socio-demographic and clinical features in patients and controls, including age, sex, handedness, education, education of the parents, duration of illness, age of onset, duration of untreated psychosis and number of hospitalizations. As a consequence of the matching process, no differences emerged between patients and controls, except for the education level ($P<001$; rb=0.74).

Of the 91 patients initially included in the study, 9 were lost on follow-up or withdrew the antipsychotic medication, thus response to treatment was only assessed in 82 subjects. Responders and non-responders to treatment showed no significant differences in any of the abovementioned variables, but the former had higher disorganized ($p = 0.017$, rb = -0.31) and excited ($p = 0.029$, rb = -0.28) scores (**table S2**).

Upon admission all the patients were drug naïve or had withdrawn antipsychotic medications, and at the moment of the EEG recording all had started a new treatment, with the exception of N=1 patient who did not receive any treatment during the hospitalization; antipsychotic medication characteristics are reported in **table 2**, and no differences emerged

between responders and non-responders concerning medication's specific active principle and category, risperidone equivalent dose at the moment of the EEG recording and after titration, with the exception of the number of subjects receiving risperidone as an add-on treatment (p=0.014, V=0.57). The duration of the ongoing treatment at the moment of the EEG recording, corresponding to the hospitalization day on whom the recording was taken, was comparable between groups (**table S2**).

Attrition bias analysis showed an attrition rate of 9.9%, and a higher number of hospitalization (p=0.042, rb=-0.41) and more severe negative symptoms (p=0.044, rb=-0.41) in patients completing the study compared to the ones lost on follow-up, with no other clinical difference between the two groups (**table S3**).

Patients present no gamma band reduction, but lower theta ITC and ERSP compared to controls

Gamma band (38-42 Hz)

No ITC differences were observed for the patients vs. controls comparison, with only a non-significant increase in gamma synchrony emerging in the early window in a few central electrodes (t=2.42, d=0.45, $N_{electrodes}$=3, p=0.090).

Patients had increased gamma band ERSP in the late window (t=2.39, d =0.43, $N_{electrodes}$=6, p=0.045), not surviving FDR correction for multiple testing, and a non statistically significant increase in the early window (t=2.34, d=0.47, $N_{electrodes}$=4, p=0.061), compared to controls. In both cases differences were localized to the frontal region (**Figure 1, table S4**).

Gamma band equivalence testing against the meta-analytic bounds suggests increased early and late ERSP and ITC in our patients cohort compared to the ones assessed in the previous literature, with present estimates being incompatible with the reduction in the pooled ones (**supplementary results**, **figures S1-2, tables S5-7**).

No differences were observed between patients completing the study and lost on follow up (attrition bias analysis), concerning gamma ITC and ERSP in the early and late windows (**table S8**).

Theta band (4-8 Hz)

Theta-band ITC was significantly reduced in patients in the early window (t=-4.17, d=-0.97, $N_{electrodes}$=22, p<.001) and in the late window (t =-2.96, d=-0.62, $N_{electrodes}$=7, p=0.024); while the difference in the early window was localized to the almost entirety of candidate electrodes, differences in the late window involved a smaller frontal cluster.

Theta-band ERSP was reduced in patients relative to controls in the early window (t=−3.58, d=−0.88, $N_{electrodes}$=20, p <.001) and in the late window (t=−2.53, d=−0.64, $N_{electrodes}$=8, p=0.013). In the early window, the difference was in a broad cluster comprising almost all the

candidate electrodes, while in the late window, a left fronto-central cluster was involved (**Figure 2; table S9**).

All the ITC and ERSP significant results resisted FDR correction for multiple testing, and the sensitivity analysis revealed no relevant influence of any of the potential confounders tested (**table S10**).

No differences were observed between patients completing the study and lost on follow up, concerning ITC and ERSP in the early and late windows (**table S11**).

Correlations with symptoms severity

Gamma band (38-42 Hz)

Gamma ITC in the early window correlated with negative symptom severity (t=2.43, ρ=0.30, $N_{electrodes}$=7, p=0.038) in a central cluster of electrodes asymmetric to the left; however, the association did not survive FDR correction for multiple testing (**figure S3**). A trend-level correlation in the same direction was observed for negative symptoms and gamma ITC in the late window, in a left-central cluster (t=2.41, ρ=0.28, $N_{electrodes}$=4, p=0.079). No significant correlations were found for the remaining subscales (disorganized, excited, depressed) or for the PANSS total score.

No significant correlations emerged between symptom dimensions and ERSP metrics in gamma band, even if a trend-level association emerged between gamma ERSP in the late window and negative symptoms (t=2.49, ρ=0.25, $N_{electrodes}$=4, p=0.069), in a left central cluster of electrodes (**table S12**).

Theta band (4-8 Hz)

Theta ITC in the late window was positively correlated with positive symptom severity (t=2.32, ρ=0.30, $N_{electrodes}$=6, p=0.043) in a central cluster of right-asymmetric electrodes (**figure S3**), an association not surviving FDR correction for multiple testing.

No significant correlations emerged concerning early window ITC and ERSP **(table S13)**.

Within patients, reduced gamma ITC and ERSP are associated with antipsychotic treatment response

Gamma band (38-42 Hz)

ITC was significantly reduced in responders compared to non-responders in the early window (t=−2.69, d=−0.64, $N_{electrodes}$=11, p=0.015) and in the late window (t=−2.66, d=−0.62, $N_{electrodes}$=10, p=0.025). Differences were localized to a symmetric fronto-central cluster of electrodes in both windows.

ERSP was also reduced in responders relative to non-responders in the late window (t=−2.37, d=−0.57, $N_{electrodes}$=9, p=0.025), in a symmetric cluster of frontal electrodes (**Figure 3, table S14**). No ERSP differences emerged in the early window.

All significant results resisted FDR correction for multiple testing and the sensitivity analysis showed no relevant attenuation due to the potential confounders tested (**table S15**).
Late gamma ITC correlated with the percentage change in symptom scores between baseline and follow-up (ρ=0.25, $N_{electrodes}$=7, p=0.047) in a frontal cluster asymmetric to the left (**figure S4**, **table S16**), however the result did not survive FDR correction for multiple testing. Early ITC and all the ERSP metrics showed no significant associations with the symptoms variation from baseline to follow-up.

Theta band (4-8 Hz)

Responders showed a trend-level decrease in early ERSP (t=.2.54, d=-0.68, $N_{electrodes}$=4, p=0.058), compared to non-responders. No significant theta-band clusters emerged for the ITC and ERSP comparisons, in the early and late windows (**figure S5, table S17**), and no theta metrics correlated with the PANSS total score change from baseline to follow-up, even if a trend-level correlation emerged with ERSP early (ρ=0.27, $N_{electrodes}$=4, p=0.070; **table S18**).

Gamma ITC and ERSP are increased in non-responders compared to controls, but not in responders

Gamma band (38-42 Hz)

No significant ITC differences emerged between responders and controls in early and late gamma (**figure S6**).
Gamma-band ITC was increased in non-responders relative to controls in the early window, localized to the majority of candidate electrodes (t=2.52, d=0.65, $N_{electrodes}$=21, p=0.002) and in the late window (t=2.50, d=0.61, $N_{electrodes}$=17, p=0.010) in a large fronto-central cluster slightly left-asymmetric (**figure 4**).

In the early window, increased gamma ERSP was observed for both responders (t=2.19, d=0.58, $N_{electrodes}$=5, p=0.048, **figure S6**) and non-responders (t=2.22, $N_{electrodes}$=7, p=0.024, d=0.57, **figure 4**), in both cases localized to a small frontal cluster. However, for responders the association did not survive FDR correction for multiple testing.
Non-responders (but not responders) also showed significantly increased gamma ERSP relative to controls in the late window (t=2.66, d=0.67, $N_{electrodes}$=15, p = 0.005), in a large symmetrical fronto-central cluster (**figure 4**, **table S19**).

All results for non-responders resisted FDR correction for multiple testing and the sensitivity analysis showed no attenuation when testing potential clinical and demographic confounders (**table S20**).

Gamma band equivalence testing against the meta-analytic bounds suggests an increased early and late ERSP and ITC compared to the previous literature in both responders and non-responders to treatment, more marked in the latter (**supplementary results**, **figure S1-2**, **tables S5-7**). For both groups the estimates in our cohort are incompatible with the pooled ones from previous literature.

Theta band (4-8 Hz)

In both ITC and ERSP we could find results overlapping with the ones on the full cohort, with statistical significance and effect size of these differences being similar for both responders and non-responders when each group was compared to controls — the only exception being the nonsignificant difference in ITC between responders and controls (**figures S7-8**, **table S21**).

Significant results were all surviving FDR correction for multiple testing, and the sensitivity analysis showed that they were not attenuated by clinical and demographic covariates (**table S22**).

Post-hoc assessment of theta activity

Findings are only summarized in the present paragraph and extensively reported in **supplementary results (figures S9-11, tables S23-26)**.

The analysis of the temporal specificity of the post onset theta response indicate the non-artifactual nature of the early window 4-8 Hz activity, that is not related to filtering nor to the edge effect.

The ERP analysis in the early window showed the existence of evoked activity corresponding to the N100 and P200 event-related potential, following stimulus onset, in both patients with schizophrenia and controls. The N100 but not the P200 mean and peak amplitudes were reduced in patients compared to controls. Mean and peak amplitudes of both ERPs showed a strong correlation with theta ITC and ERSP in the early window. However, introducing N1 and P2 mean amplitude as covariates partly attenuated but did not abolish these differences between groups ASSR parameters in the early window theta, that remained highly significant and with a medium-to-large effect size. Moreover, the sensitivity analysis showed no relevant influence of any confounders on significance and effect size of these group differences.

An analysis on the partition of the theta activity revealed that in the early window most of the theta activity was evoked (63.2% in patients, 75.3% in controls), yet with a large induced component (36.8% in patients, 24.7% in controls), while in the late window induced activity predominates.

DISCUSSION

Our study elucidated ASSR power and phase synchrony dynamics in patients with schizophrenia having an acute psychotic episode, and assessed the role of the ASSR as a predictive biomarker of the response to antipsychotic medications. Main results are: no statistically significant differences in gamma band ERSP and ITC between patients and controls, but an increase of both in the subgroup of non-responders to treatment, compared to controls; reduced theta power (ERSP) and synchrony (ITC) in patients compared to controls; reduced gamma ITC and late ERSP in responders compared to non-responders to treatment

Therefore, acute patients with schizophrenia presented no reduction in gamma band activity compared to controls, in contrast with our initial hypothesis and with the established literature, that showed decreased ERSP and ITC in schizophrenia with moderate to large effect size (g=-0.702 for ERSP and g=-0.897 for ITC) (15), with only few studies finding no differences in patients vs controls (34-37), or an increased gamma power (38).

Subjects entering past studies were typically outpatients stabilized under an effective and long-standing antipsychotic treatment, different from the ones in our minimally treated, hospitalized cohort; we hypothesize that the observed findings on gamma ERSP and ITC result from a compensatory process especially active during the acute phase of schizophrenia and corresponding to a different E/I imbalance and NMDA receptor dysregulation compared to what is observed in stabilized outpatients.

A reduced excitatory state of the cerebral cortex is regarded as the fundamental pathophysiological mechanisms of schizophrenia (39, 40), due to a primary loss of excitability of the cortical pyramidal neurons, reflecting hypofunction of NMDA receptors and their signaling cascade. Reduced excitatory input to inhibitory PV-interneurons would then lead to their compensatory downregulation, in an attempt to restore the E/I balance (39, 41-43).

Our post-hoc interpretation is that the pathophysiology process leading to PV-interneurons downregulation is especially active during the acute phase of the disease, as supported by computational modeling studies, indicating that the PV-interneuron downregulation is a compensatory process positively correlated with gamma band activity (39, 41, 43-45), and leading to positive (43) and negative (44) symptoms, that are more expressed in the acute phase of the disease. While the pyramidal neuron downregulation would correspond to a decrease in ASSR gamma band activity, the PV-interneurons downregulation would raise patients' gamma activity to a level similar to controls, as indicated by both ERSP and ITC values. Subgroup analysis discussed below clarified that non-responders to treatment (but

not responders) had an increase in ITC gamma compared to controls, potentially due to an especially strong expression of the PV-interneuron downregulation process.

We complemented conventional significance testing of the gamma-band contrasts with equivalence testing against the effect size reported meta-analytically, evidencing that our results are incompatible with the gamma band ITC and ERSP reduction in patients entering previous studies. These results indicate that pooled estimates derived from stabilized outpatients do not generalize to the acute phase, whose gamma band activity could be comparatively increased.

Our results added some limited pieces of knowledge to the dimensional psychopathology of schizophrenia and its biological underpinnings. We have observed a positive correlation between negative symptoms and gamma ITC, and between positive symptoms and theta ITC, although not surviving correction for multiple testing. The loss of significance in our results likely reflects the restricted variance of our acutely psychotic cohort, who are clinically homogeneous — especially for positive symptoms — limiting the range required to detect associations between clinical and neurophysiological measures.

Interesting findings, not a focus of previous ASSR studies, concerned theta band ERSP and ITC, which differentiate patients and controls with high effect size. In fact, the latter displayed a theta activity peak at the onset of the auditory stimulation (0-0.25s), then persisting with lower intensity in the late window (0.25-1.25s); both were markedly decreased in patients. This reduction was partially expected, because compatible with an oscillatory expression of the well-documented attenuation of the auditory N1–P2 complex in schizophrenia (46-48). However, our analyses indicate that, while a part of the early theta response is phase-locked to stimulus onset, thus reflecting the low-frequency content of the auditory evoked response, another relevant part corresponds to induced activity or to evoked activity not related to the N1-P2 complex. Therefore, the ASSR stimulation triggers a specific activity in the theta band, sustained to the late window, and impaired in schizophrenia.
These results are relevant, because they contribute to the characterization of the theta activity in schizophrenia, that is a solid neurophysiological marker, consistently increased in the resting-state in chronic (24-26) and first episode (49) schizophrenia, also including patients' probands (50). Resting-state theta increase was related to reduced cognitive control/inhibition (27), and to a more severe cognitive impairment (28, 29), especially involving working memory and attention (51), corroborating its relevance. In conclusion, theta dysregulation in schizophrenia would consist of an increased resting-state activity (as for past literature) and of a reduced task-induced activity (as for our findings), echoing the

classical pattern described for gamma band (13), and representing a mechanistic insight into perceptual impairment in schizophrenia.

Concerning response to treatment, non-responders had significantly increased gamma ITC and late ERSP compared to non-responders. Our interpretation is that the two groups are differentiated by the extent of the compensatory PV-interneuron downregulation process mentioned above: the more the process is active, the less the antipsychotic medications are able to restore an appropriate E/I balance, perhaps because they mainly act on the loss of excitability of the pyramidal neuron. In fact antipsychotic medications have no direct influence on glutamatergic or GABAergic system whose receptor localize to PV interneurons; on the contrary, they can affect pyramidal neuron activity directly, by binding to the serotonin receptors on their soma (52), and indirectly, affecting the cortico-striatal-thalamic-cortical loops through dopaminergic antagonism (53-56).
Besides assessing response to treatment as a binary outcome, we have also examined the correlation between ASSR parameters and the PANSS total score change between the baseline and the follow-up visit, leading to weak results, only concerning the late gamma ITC, not resisting correction for multiple testing. A possible explanation is that the relationship between ASSR and treatment outcome may be closer to a threshold than a gradient: ASSR may index membership of a treatment-responsive phenotype without scaling with the magnitude of symptom change, in which case a group contrast can be significant while a linear correlation is not.

When assessing responders and non-responders separately against controls, non-responders only presented a statistically significant increase in gamma ERSP and ITPC, lending support to the role of these ASSR changes in gamma band as specific predictors of non-response to treatment.
These findings provide pieces of knowledge to the growing trend that different group of patients with psychosis exist, corresponding to biotypes with different clinical and neurophysiological features (57), and gives hints on how clustering could lead to relevant clinical decisions, such as the treatment of patients with poorer clinical trajectory.
Only two previous study exist dealing with antipsychotic treatment outcome and ASSR, though not designed to define predictors, but being a comparison of stabilized outpatients. First, Ogyu compared patients with or without treatment resistant schizophrenia (TRS, i.e.: the failure to respond to ≥ 2 different non-clozapine antipsychotic medications), showing that ERSP was lower in TRS compared to controls, but not in non-TRS compared to controls; the categorization of patients (i.e. TRS vs non-TRS) and the phase of the disease (i.e. not acute) were not overlapping to the ours, making results difficult to compare (58). Second, Alegre compared acute drug naïve and well-stabilized patients under medication, concluding that

antipsychotic medications can rescue gamma-band activity in patients with schizophrenia. In fact, drug-naive patients had reduced amplitude and inter-trial phase coherence of the response in the 30–50 Hz range, and reduced amplitude of the response in the 90–100 Hz range, when compared to controls. In the treated group, the response in the 30–50 Hz range was normalized to values similar to the control group (59). The medication-induced recovery of a physiological level of gamma activity during the ASSR is a hypothesis not supported by the rest of the literature, considering that most of the patients entering previous studies were treated and well stabilized, yet showing a consistent decrease in ERSP and ITC.

Previous investigations exist on EEG-based prediction of response to antipsychotics, mostly focused on resting state power spectra, being not directly comparable with our task-related results. Only two investigations produced evidence on resting-state gamma frequencies, indicating that both a reduced (60) or an increased (61) gamma power predicts a better response, with a third study addressing the issue found no significant results (62).

The amount of clinical and preclinical evidence demonstrating the relevance of gamma activity for the pathophysiology of schizophrenia (8), could favor ASSR as a biomarker in face of alternatives without a strong biological rationale. The moderate effect size of the difference between responders and non-responders and between non-responders and controls however tempers the expectations that ASSR parameters could be translated to the clinical practice as a standalone biomarker, even if they could be more effectively used as part of an algorithm integrating several neuroimaging and plasma biomarkers, as well as clinical parameters (5, 63, 64).

Limitations

Some of our methodological choices differed from previous investigations, limiting direct comparisons: Factors associated with a stronger ASSR concerning power and phase are the younger age, the lower stimulus duration and the attentional load. This could explain a weaker effect in our study, where the average age was higher than previous cohorts, the stimulus duration long and no active engagement of the patient was required, to permit acute patients to participate more easily (14, 15). However, only long and modulated stimuli are appropriate to obtain a specific and sustained entrainment truly corresponding to the nature of a steady state response, while protocols based on other stimuli type are prone to capture aspecific transient activity.

We had no EEG recording during the follow-up visit, which could clarify if antipsychotic treatment would normalize brain dynamics during the acute psychotic episode, and if in a stabilized state our cohort of patients mirrors meta-analytic findings on other outpatients cohort. However, our study was primarily designed to assess the acute phase of schizophrenia and discover predictors of response to antipsychotic medications, not to

define the trajectory of EEG features in the course of the illness.

Another inherent limitation of the study is the lack of a long-term assessment of a sustained response to medication; however, the design of our study was aligned with the normal duration of clinical trials, of 4 to 12 weeks (65-67).

Last, patients were included within 72h of hospital admission, having already received initial doses of treatment. This approach significantly improved feasibility and we believe it had minimal potential for bias, as evidence suggests that 6–10 days are required for antipsychotic effects to become clinically significant (66, 68, 69).

CONCLUSIONS

During an acute episode, compared to controls, patients with schizophrenia present a peculiar ASSR pattern with reduced theta and normal-to-increased gamma, different from what has been observed in previous studies on stabilized outpatients. This could possibly reflect an interplay between pyramidal neuron and PV-interneurons E/I imbalance that is specific to this clinical frame.

Our findings support the existence of a neurobiological difference between responders and non-responders to antipsychotic treatment, with the latter having increased gamma band activity in the acute phase, also compared to controls. These findings open avenues to the possibility that the ASSR becomes a predictive biomarker for the stratification of treatment outcome, more likely as part of an algorithm combining several clinical and instrumental measures.

DECLARATION OF INTEREST

Stefan Kaiser received advisory board honoraria from Boehringer and Exeltis as well as royalties for cognitive test and training softwares from Schuhfried. Matthias Kirschner received advisory board honoraria from Otsuka. The other authors declare no competing interest.

ACKNOWLEDGMENTS

The work was financially supported by the foundation Jean and Madeleine Vachoux of Geneva and by the Research and Development program (PRD) of the Geneva University hospital (HUG).

SUPPLEMENTARY MATERIALS

Supplementary information is available at Molecular Psychiatry website

DATA AVAILABILITY STATEMENT

Clinical and EEG datasets are available upon request.

REFERENCES

1. Haddad PM, Correll CU. The acute efficacy of antipsychotics in schizophrenia: a review of recent meta-analyses. Ther Adv Psychopharmacol. 2018;8(11):303-18.
2. Lieberman JA, Stroup TS, McEvoy JP, Swartz MS, Rosenheck RA, Perkins DO, et al. Effectiveness of antipsychotic drugs in patients with chronic schizophrenia. N Engl J Med. 2005;353(12):1209-23.
3. Perkovic MN, Erjavec GN, Strac DS, Uzun S, Kozumplik O, Pivac N. Theranostic Biomarkers for Schizophrenia. Int J Mol Sci. 2017;18(4).
4. Lai CY, Scarr E, Udawela M, Everall I, Chen WJ, Dean B. Biomarkers in schizophrenia: A focus on blood based diagnostics and theranostics. World J Psychiatry. 2016;6(1):102-17.
5. Carbon M, Correll CU. Clinical predictors of therapeutic response to antipsychotics in schizophrenia. Dialogues Clin Neurosci. 2014;16(4):505-24.
6. McCutcheon RA, Reis Marques T, Howes OD. Schizophrenia-An Overview. JAMA Psychiatry. 2020;77(2):201-10.
7. De Pieri M, Rochas V, Sabe M, Michel C, Kaiser S. Pharmaco-EEG of antipsychotic treatment response: a systematic review. Schizophrenia (Heidelb). 2023;9(1):85.
8. McNally JM, McCarley RW. Gamma band oscillations: a key to understanding schizophrenia symptoms and neural circuit abnormalities. Curr Opin Psychiatry. 2016;29(3):202-10.
9. Uhlhaas PJ, Singer W. Neuronal dynamics and neuropsychiatric disorders: toward a translational paradigm for dysfunctional large-scale networks. Neuron. 2012;75(6):963-80.
10. Buzsaki G, Wang XJ. Mechanisms of gamma oscillations. Annu Rev Neurosci. 2012;35:203-25.
11. Fernandez-Ruiz A, Sirota A, Lopes-dos-Santos V, Dupret D. Over and above frequency: Gamma oscillations as units of neural circuit operations. Neuron. 2023;111(7):936-53.
12. Sohal VS. Transforming Discoveries About Cortical Microcircuits and Gamma Oscillations Into New Treatments for Cognitive Deficits in Schizophrenia. Am J Psychiatry. 2022;179(4):267-76.
13. De Pieri M, Sabe M, Rochas V, Poglia G, Bartolomei J, Kirschner M, et al. Resting-state EEG and MEG gamma frequencies in schizophrenia: a systematic review and exploratory power-spectrum metanalysis. Schizophrenia (Heidelb). 2025;11(1):48.
14. Thune H, Recasens M, Uhlhaas PJ. The 40-Hz Auditory Steady-State Response in Patients With Schizophrenia: A Meta-analysis. JAMA Psychiatry. 2016;73(11):1145-53.
15. Kinjo M, Tamura S, Sugiyama S, van Weert E, Oribe N, Tsuchimoto R, et al. A systematic review and meta-analysis of the auditory steady-state response in schizophrenia, bipolar disorder, and autism spectrum disorder. Mol Psychiatry. 2026;31(6):3169-75.
16. Zouaoui I, Dumais A, Lavoie ME, Potvin S. Auditory Steady-State Responses in Schizophrenia: An Updated Meta-Analysis. Brain Sci. 2023;13(12).

17. Grent-'t-Jong T, Brickwedde M, Metzner C, Uhlhaas PJ. 40-Hz Auditory Steady-State Responses in Schizophrenia: Toward a Mechanistic Biomarker for Circuit Dysfunctions and Early Detection and Diagnosis. Biol Psychiatry. 2023;94(7):550-60.
18. Kwon JS, O'Donnell BF, Wallenstein GV, Greene RW, Hirayasu Y, Nestor PG, et al. Gamma frequency-range abnormalities to auditory stimulation in schizophrenia. Arch Gen Psychiatry. 1999;56(11):1001-5.
19. Liu Y, Ouyang P, Zheng Y, Mi L, Zhao J, Ning Y, et al. A Selective Review of the Excitatory-Inhibitory Imbalance in Schizophrenia: Underlying Biology, Genetics, Microcircuits, and Symptoms. Front Cell Dev Biol. 2021;9:664535.
20. Howes OD, Shatalina E. Integrating the Neurodevelopmental and Dopamine Hypotheses of Schizophrenia and the Role of Cortical Excitation-Inhibition Balance. Biol Psychiatry. 2022;92(6):501-13.
21. Grent-'t-Jong T, Gajwani R, Gross J, Gumley AI, Krishnadas R, Lawrie SM, et al. 40-Hz Auditory Steady-State Responses Characterize Circuit Dysfunctions and Predict Clinical Outcomes in Clinical High-Risk for Psychosis Participants: A Magnetoencephalography Study. Biol Psychiatry. 2021;90(6):419-29.
22. Murphy N, Ramakrishnan N, Walker CP, Polizzotto NR, Cho R. Intact Auditory Cortical Cross-Frequency Coupling in Early and Chronic Schizophrenia. Biological Psychiatry. 2020;87(9).
23. Edgar JC, Chen YH, Lanza M, Howell B, Chow VY, Heiken K, et al. Cortical thickness as a contributor to abnormal oscillations in schizophrenia? Neuroimage Clin. 2014;4:122-9.
24. Adams RA, Bush D, Zheng F, Meyer SS, Kaplan R, Orfanos S, et al. Impaired theta phase coupling underlies frontotemporal dysconnectivity in schizophrenia. Brain. 2020;143(4):1261-77.
25. Hunt MJ, Kopell NJ, Traub RD, Whittington MA. Aberrant Network Activity in Schizophrenia. Trends Neurosci. 2017;40(6):371-82.
26. Newson JJ, Thiagarajan TC. EEG Frequency Bands in Psychiatric Disorders: A Review of Resting State Studies. Front Hum Neurosci. 2018;12:521.
27. Eisma J, Rawls E, Long S, Mach R, Lamm C. Frontal midline theta differentiates separate cognitive control strategies while still generalizing the need for cognitive control. Sci Rep. 2021;11(1):14641.
28. Cao Y, Han C, Peng X, Su Z, Liu G, Xie Y, et al. Correlation Between Resting Theta Power and Cognitive Performance in Patients With Schizophrenia. Front Hum Neurosci. 2022;16:853994.
29. Tan E, Troller-Renfree SV, Morales S, Buzzell GA, McSweeney M, Antunez M, et al. Theta activity and cognitive functioning: Integrating evidence from resting-state and task-related developmental electroencephalography (EEG) research. Dev Cogn Neurosci. 2024;67:101404.
30. Wallwork RS, Fortgang R, Hashimoto R, Weinberger DR, Dickinson D. Searching for a consensus five-factor model of the Positive and Negative Syndrome Scale for schizophrenia. Schizophr Res. 2012;137(1-3):246-50.
31. Leucht S, Davis JM, Engel RR, Kissling W, Kane JM. Definitions of response and remission in schizophrenia: recommendations for their use and their presentation. Acta Psychiatr Scand Suppl. 2009(438):7-14.

610 32. McCutcheon RA, Pillinger T, Mizuno Y, Montgomery A, Pandian H, Vano L, et al.
611 The efficacy and heterogeneity of antipsychotic response in schizophrenia: A meta-
612 analysis. Mol Psychiatry. 2021;26(4):1310-20.
613 33. Lakens D. Equivalence Tests: A Practical Primer for t Tests, Correlations, and
614 Meta-Analyses. Soc Psychol Personal Sci. 2017;8(4):355-62.
615 34. Hong LE, Summerfelt A, McMahon R, Adami H, Francis G, Elliott A, et al. Evoked
616 gamma band synchronization and the liability for schizophrenia. Schizophr Res.
617 2004;70(2-3):293-302.
618 35. Hirano Y, Oribe N, Kanba S, Onitsuka T, Nestor PG, Spencer KM. Spontaneous
619 Gamma Activity in Schizophrenia. JAMA Psychiatry. 2015;72(8):813-21.
620 36. Rass O, Forsyth JK, Krishnan GP, Hetrick WP, Klaunig MJ, Breier A, et al. Auditory
621 steady state response in the schizophrenia, first-degree relatives, and schizotypal
622 personality disorder. Schizophr Res. 2012;136(1-3):143-9.
623 37. Hamm JP, Gilmore CS, Picchetti NA, Sponheim SR, Clementz BA. Abnormalities
624 of neuronal oscillations and temporal integration to low- and high-frequency auditory
625 stimulation in schizophrenia. Biol Psychiatry. 2011;69(10):989-96.
626 38. Kim S, Jang SK, Kim DW, Shim M, Kim YW, Im CH, et al. Cortical volume and 40-
627 Hz auditory-steady-state responses in patients with schizophrenia and healthy controls.
628 Neuroimage Clin. 2019;22:101732.
629 39. Krystal JH, Anticevic A, Yang GJ, Dragoi G, Driesen NR, Wang XJ, et al. Impaired
630 Tuning of Neural Ensembles and the Pathophysiology of Schizophrenia: A Translational
631 and Computational Neuroscience Perspective. Biol Psychiatry. 2017;81(10):874-85.
632 40. Stephan KE, Friston KJ, Frith CD. Dysconnection in schizophrenia: from
633 abnormal synaptic plasticity to failures of self-monitoring. Schizophr Bull.
634 2009;35(3):509-27.
635 41. Chung DW, Fish KN, Lewis DA. Pathological Basis for Deficient Excitatory Drive to
636 Cortical Parvalbumin Interneurons in Schizophrenia. Am J Psychiatry.
637 2016;173(11):1131-9.
638 42. Dienel SJ, Lewis DA. Alterations in cortical interneurons and cognitive function in
639 schizophrenia. Neurobiol Dis. 2019;131:104208.
640 43. Adams RA, Pinotsis D, Tsirlis K, Unruh L, Mahajan A, Horas AM, et al.
641 Computational Modeling of Electroencephalography and Functional Magnetic
642 Resonance Imaging Paradigms Indicates a Consistent Loss of Pyramidal Cell Synaptic
643 Gain in Schizophrenia. Biol Psychiatry. 2022;91(2):202-15.
644 44. Shaw AD, Knight L, Freeman TCA, Williams GM, Moran RJ, Friston KJ, et al.
645 Oscillatory, Computational, and Behavioral Evidence for Impaired GABAergic Inhibition
646 in Schizophrenia. Schizophr Bull. 2020;46(2):345-53.
647 45. Wengler K, Goldberg AT, Chahine G, Horga G. Distinct hierarchical alterations of
648 intrinsic neural timescales account for different manifestations of psychosis. Elife.
649 2020;9.
650 46. Salisbury DF, Collins KC, McCarley RW. Reductions in the N1 and P2 auditory
651 event-related potentials in first-hospitalized and chronic schizophrenia. Schizophr Bull.
652 2010;36(5):991-1000.
653 47. Wang B, Zartaloudi E, Linden JF, Bramon E. Neurophysiology in psychosis: The
654 quest for disease biomarkers. Transl Psychiatry. 2022;12(1):100.
655 48. Rosburg T. Auditory N100 gating in patients with schizophrenia: A systematic
656 meta-analysis. Clin Neurophysiol. 2018;129(10):2099-111.

49. Koenig T, Lehmann D, Saito N, Kuginuki T, Kinoshita T, Koukkou M. Decreased functional connectivity of EEG theta-frequency activity in first-episode, neuroleptic-naive patients with schizophrenia: preliminary results. Schizophr Res. 2001;50(1-2):55-60.
50. Narayanan B, O'Neil K, Berwise C, Stevens MC, Calhoun VD, Clementz BA, et al. Resting state electroencephalogram oscillatory abnormalities in schizophrenia and psychotic bipolar patients and their relatives from the bipolar and schizophrenia network on intermediate phenotypes study. Biol Psychiatry. 2014;76(6):456-65.
51. Cavanagh JF, Frank MJ. Frontal theta as a mechanism for cognitive control. Trends Cogn Sci. 2014;18(8):414-21.
52. Stahl SM. Beyond the dopamine hypothesis of schizophrenia to three neural networks of psychosis: dopamine, serotonin, and glutamate. CNS Spectr. 2018;23(3):187-91.
53. Surmeier DJ, Carrillo-Reid L, Bargas J. Dopaminergic modulation of striatal neurons, circuits, and assemblies. Neuroscience. 2011;198:3-18.
54. Brandalise F, Chereau R, Chen IW, van Oorschot D, Morin Raig C, Bawa T, et al. Thalamocortical feedback selectively controls pyramidal neuron excitability. Nat Commun. 2025;16(1):5663.
55. Sherman SM, Guillery RW. The role of the thalamus in the flow of information to the cortex. Philos Trans R Soc Lond B Biol Sci. 2002;357(1428):1695-708.
56. Douglas RJ, Martin KA. Neuronal circuits of the neocortex. Annu Rev Neurosci. 2004;27:419-51.
57. Clementz BA, Parker DA, Trotti RL, McDowell JE, Keedy SK, Keshavan MS, et al. Psychosis Biotypes: Replication and Validation from the B-SNIP Consortium. Schizophr Bull. 2022;48(1):56-68.
58. Ogyu K, Matsushita K, Honda S, Wada M, Tamura S, Takenouchi K, et al. Decrease in gamma-band auditory steady-state response in patients with treatment-resistant schizophrenia. Schizophr Res. 2023;252:129-37.
59. Alegre M, Molero P, Valencia M, Mayner G, Ortuno F, Artieda J. Atypical antipsychotics normalize low-gamma evoked oscillations in patients with schizophrenia. Psychiatry Res. 2017;247:214-21.
60. Arikan MK, Gunver G, Ilhan R, Oksuz O, Metin B. Gamma oscillations predict treatment response to aripiprazole in bipolar disorder. J Affect Disord. 2021;294:159-62.
61. Itil TM, Shapiro D, Schneider SJ, Francis IB. Computerized EEG as a predictor of drug response in treatment resistant schizophrenics. J Nerv Ment Dis. 1981;169(10):629-37.
62. Mitra S, Nizamie SH, Goyal N, Tikka SK. Evaluation of resting state gamma power as a response marker in schizophrenia. Psychiatry Clin Neurosci. 2015;69(10):630-9.
63. Ricci V, Sarni A, Barresi M, Remondino L, Martinotti G, Maina G. Biomarkers for Predicting Clinical Deterioration in Schizophrenia-Spectrum Disorders: A Systematic Review. Brain Sci. 2026;16(6).
64. Abi-Dargham A, Moeller SJ, Ali F, DeLorenzo C, Domschke K, Horga G, et al. Candidate biomarkers in psychiatric disorders: state of the field. World Psychiatry. 2023;22(2):236-62.
65. Leucht S, Cipriani A, Spineli L, Mavridis D, Orey D, Richter F, et al. Comparative efficacy and tolerability of 15 antipsychotic drugs in schizophrenia: a multiple-treatments meta-analysis. Lancet. 2013;382(9896):951-62.

66. Agid O, Kapur S, Arenovich T, Zipursky RB. Delayed-onset hypothesis of antipsychotic action: a hypothesis tested and rejected. Arch Gen Psychiatry. 2003;60(12):1228-35.
67. Huhn M, Nikolakopoulou A, Schneider-Thoma J, Krause M, Samara M, Peter N, et al. Comparative efficacy and tolerability of 32 oral antipsychotics for the acute treatment of adults with multi-episode schizophrenia: a systematic review and network meta-analysis. Lancet. 2019;394(10202):939-51.
68. Suzuki T, Remington G, Arenovich T, Uchida H, Agid O, Graff-Guerrero A, et al. Time course of improvement with antipsychotic medication in treatment-resistant schizophrenia. Br J Psychiatry. 2011;199(4):275-80.
69. Levine SZ, Leucht S. Delayed- and early-onset hypotheses of antipsychotic drug action in the negative symptoms of schizophrenia. Eur Neuropsychopharmacol. 2012;22(11):812-7.

FIGURES TITLE AND CAPTION

Figure 1: **Gamma-band (38-42 Hz) event related spectral perturbation (ERSP) and intertrial phase coherence (ITC) in patients vs controls.**

Panels show group comparisons for ITC (**A**, **B**) and ERSP (**C**, **D**) in the early (0–0.25 s; **A**, **C**) and late (0.25–1.25 s; **B**, **D**) post-stimulus windows, including grand-average Time-Frequency Representations (TFRs) of baseline-corrected power (Decibel) or phase locking factor, spatial distribution and statistical group comparisons.

Figure 2: **Theta-band (4-8 Hz) event related spectral perturbation (ERSP) and intertrial phase coherence (ITC) in patients vs controls.**

Panels show group comparisons for ITC (**A**, **B**) and ERSP (**C**, **D**) in the early (0–0.25 s; **A**, **C**) and late (0.25–1.25 s; **B**, **D**) post-stimulus windows, including grand-average Time-Frequency Representations (TFRs) of baseline-corrected power (Decibel; **C**, **D**) or phase locking factor (**A, B**), spatial distribution and statistical group comparisons.

Figure 3: **Gamma-band (38-42 Hz) event related spectral perturbation (ERSP) and intertrial phase coherence (ITC) in responders vs non-responders to treatment.**

Panels show group comparisons for ITC (**A**, **B**) and ERSP (**C**, **D**) in the early (0–0.25 s; **A**, **C**) and late (0.25–1.25 s; **B**, **D**) post-stimulus windows, including grand-average Time-Frequency Representations (TFRs) of baseline-corrected power (Decibel; **C**, **D**) or phase locking factor (**A, B**), spatial distribution and statistical group comparisons.

Figure 4: **Gamma-band (38-42 Hz) event related spectral perturbation (ERSP) and intertrial phase coherence (ITC) in non-responders to treatment vs controls.**

Panels show group comparisons for ITC (**A**, **B**) and ERSP (**C**, **D**) in the early (0–0.25 s; **A**, **C**) and late (0.25–1.25 s; **B**, **D**) post-stimulus windows, including grand-average Time-Frequency Representations (TFRs) of baseline-corrected power (Decibel; **C**, **D**) or phase locking factor (**A, B**), spatial distribution and statistical group comparisons.

Supplementary figure S1: **Equivalence testing: Gamma-band effect sizes for the twelve case–control contrasts.** Positive d means the first-named group is higher. The solid vertical line marks the meta-analytic bound for inter-trial phase coherence (ITC, g = −0.897) and the dashed line that for event-related spectral perturbation (ERSP, g = −0.702); the dotted line marks zero. Intervals lying entirely above the applicable bound are drawn in green and establish non-inferiority; none is drawn in red here, as all twelve exclude their bound. Circles denote values computed over the electrodes of a significant or sub-threshold cluster; squares denote the three contrasts in which no cluster formed (responders versus controls, ITC), for which the average over all 26 region-of-interest electrodes is shown. Early = 0–0.25 s and late = 0.25–1.25 s post-stimulus. Intervals are 90%, the width matched to the two one-sided tests at α = 0.05; they are not a two-sided significance test against zero, and an interval clear of zero corresponds to $p < 0.10$ rather than $p < 0.05$.

Supplementary figure S2: **Robustness of the gamma ITC non-inferiority claim to a smaller true effect.**

Non-inferiority t statistic as a function of the assumed true d, for the early-window comparison of patients with controls. The horizontal dashed line is the rejection threshold (t = 1.66), and the vertical dotted line marks the value below which the bound is no longer excluded (d ≈ −0.60). Filled points are the observed early and late estimates.

Supplementary Figure S3: **Associations between auditory steady-state response (ASSR) measures and symptom severity.**

Association plot (Spearman correlation) and spatial distribution for negative symptoms and early window (0-0.25s) gamma (**Panel A**), and for positive symptoms and late window (0.25-1.25s) theta (**Panel B**).

Supplementary Figure S4: **Associations between gamma ITC and total PANSS score change from baseline to follow-up.**

Association plot (Spearman correlation) and spatial distribution for the significant (not surviving FDR correction for multiple testing) PANSS total score variation from baseline to follow-up and late window (0.25-1.25s) gamma band ITC (phase locking factor).

Supplementary Figure S5: **Theta-band (4-8 Hz) event related spectral perturbation (ERSP) and intertrial phase coherence (ITC) in responders vs non-responders to treatment.**

Panels show group comparisons for ITC (**A**, **B**) and ERSP (**C**, **D**) in the early (0–0.25 s; **A**, **C**) and late (0.25–1.25 s; **B**, **D**) post-stimulus windows, including grand-average Time-Frequency Representations (TFRs) of baseline-corrected power (Decibel) or phase locking factor, spatial distribution and statistical group comparisons.

Supplementary Figure S6: **Gamma-band (38-42 Hz) event related spectral perturbation (ERSP) and intertrial phase coherence (ITC) in responders to treatment vs controls.**

Panels show group comparisons for ITC (**A**, **B**) and ERSP (**C**, **D**) in the early (0–0.25 s; **A**, **C**) and late (0.25–1.25 s; **B**, **D**) post-stimulus windows, including grand-average Time-

Frequency Representations (TFRs) of baseline-corrected power (Decibel) or phase locking factor, spatial distribution and statistical group comparisons.

Supplementary Figure S7: **Theta-band (4-8 Hz) event related spectral perturbation (ERSP) and intertrial phase coherence (ITC) in responders to treatment vs controls.**

Panels show group comparisons for ITC (**A**, **B**) and ERSP (**C**, **D**) in the early (0–0.25 s; **A**, **C**) and late (0.25–1.25 s; **B**, **D**) post-stimulus windows, including grand-average Time-Frequency Representations (TFRs) of baseline-corrected power (Decibel) or phase locking factor, spatial distribution and statistical group comparisons.

Supplementary figure S8: **Theta-band (4-8 Hz) event related spectral perturbation (ERSP) and intertrial phase coherence (ITC) in non-responders to treatment vs controls.**

Panels show group comparisons for ITC (**A**, **B**) and ERSP (**C**, **D**) in the early (0–0.25 s; **A**, **C**) and late (0.25–1.25 s; **B**, **D**) post-stimulus windows, including grand-average Time-Frequency Representations (TFRs) of baseline-corrected power (Decibel) or phase locking factor, spatial distribution and statistical group comparisons.

Supplementary figure S9: **wavelength control for the post-onset theta decay.**

Baseline-corrected theta power averaged across analysed electrodes and across the theta band (4-8 Hz), computed with four Morlet wavelet parameterisations: fixed n = 3, 5 and 7 cycles, and the frequency-dependent scheme used in the main analysis ($n = f/2$, floored at 3). Time–frequency decomposition used a theta-focused frequency axis (4–12 Hz, 0.5 Hz steps) so that no wavelet exceeded the 3 s epoch.

The shaded red region in each panel spans ±2 SD at the theta centre frequency (i.e. the interval over which a strictly instantaneous event would be smeared by the wavelet alone). Panel titles give the SD at theta centre for each scheme.

Supplementary figure S10: **theta onset comparison with causal and non-causal filtering.**

Theta-band Hilbert envelopes, averaged across analysed electrodes and normalised to the pre-stimulus baseline (−0.5 to −0.1 s), obtained with a non-causal zero-phase filter (blue) and a causal minimum-phase filter (orange), applied to the continuous recording before epoching.

The shaded red region marks the pre-onset window (−0.2 to 0 s) in which backward leakage would appear. Filled circles mark the envelope peak within the 0–1 s search window, with peak latencies annotated; the grey arrow indicates the latency shift between filters.

Supplementary figure S11: **N1-P2 complex in the early time window (0-0.25 ms), in patients vs controls.**

Blue shaded region indicates N1, orange indicates P2.

N100 and P200 waveforms (**panel A**), topographies (**panel B**), mean amplitude, peak amplitude and latency values (**panel C**) in patients vs controls.

Figure 1

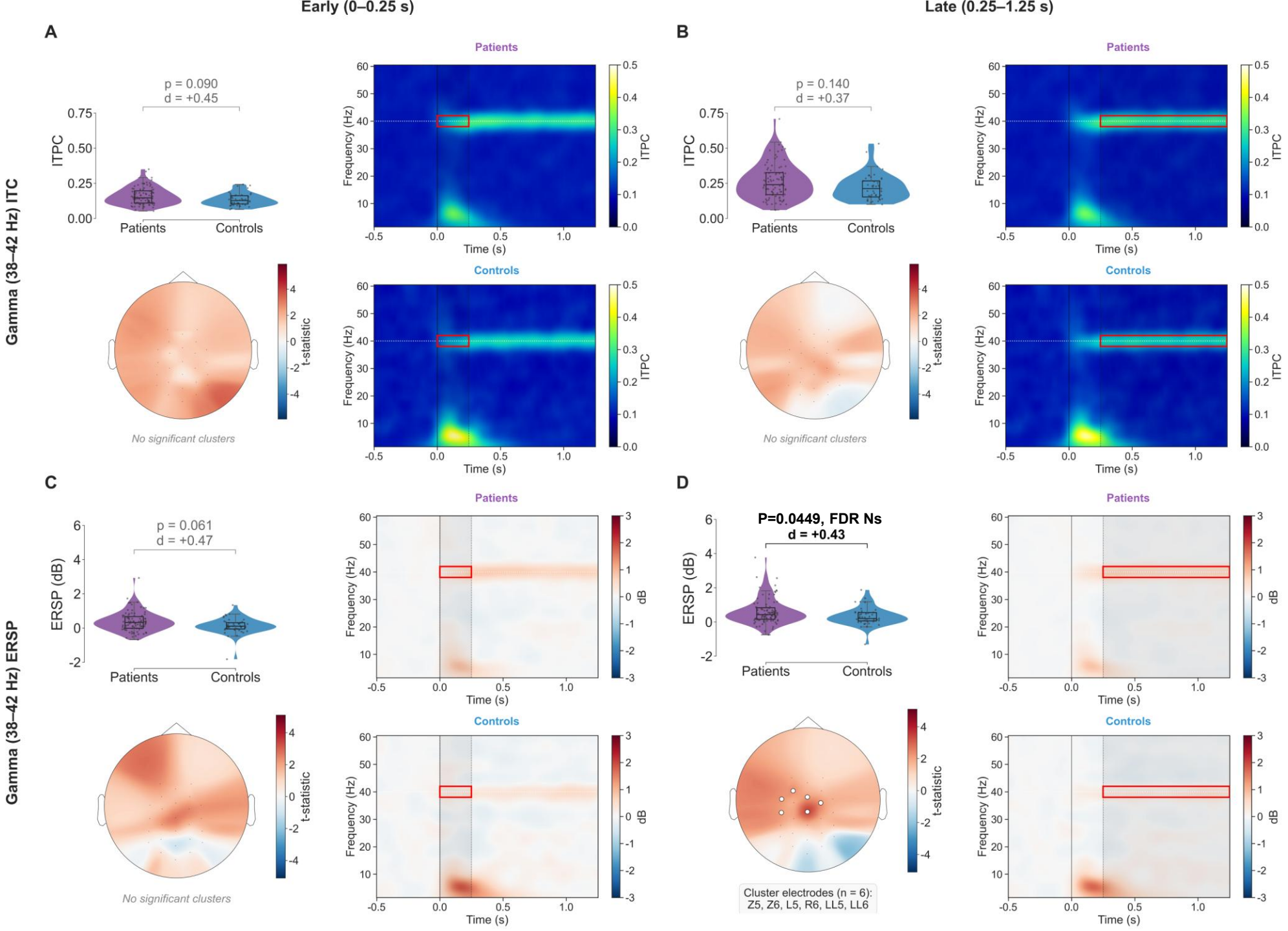

Early (0–0.25 s)
Late (0.25–1.25 s)
A
B
C
D
Gamma (38–42 Hz) ITC
Gamma (38–42 Hz) ERSP
p = 0.090
d = +0.45
p = 0.140
d = +0.37
p = 0.061
d = +0.47
P=0.0449, FDR Ns
d = +0.43
ITPC
ERSP (dB)
Patients
Controls
Frequency (Hz)
Time (s)
t-statistic
dB
No significant clusters
Cluster electrodes (n = 6):
Z5, Z6, L5, R6, LL5, LL6

Figure 2

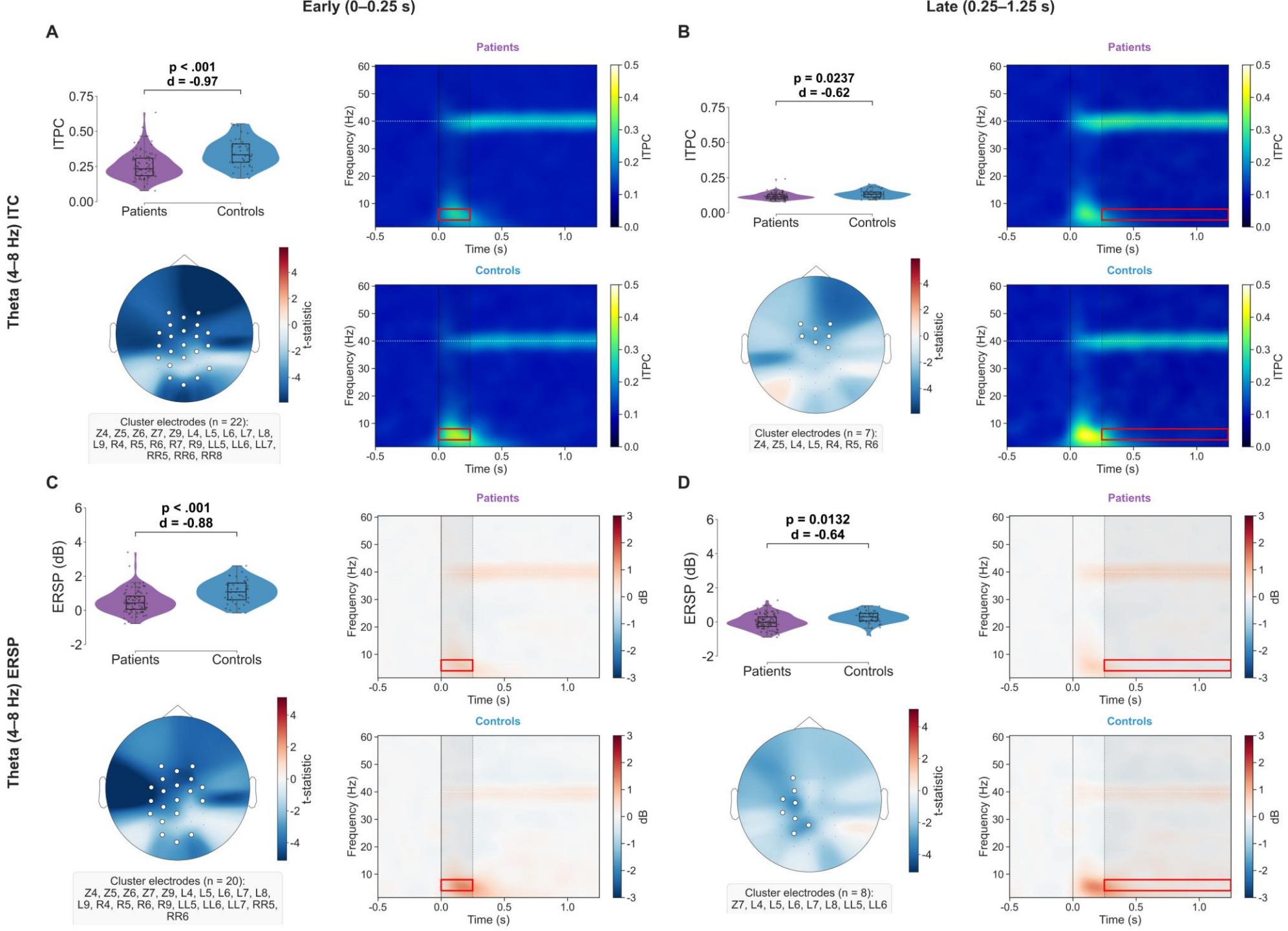

Early (0–0.25 s)
Late (0.25–1.25 s)
A
B
C
D
Theta (4–8 Hz) ITC
Theta (4–8 Hz) ERSP
p < .001
d = -0.97
p = 0.0237
d = -0.62
p < .001
d = -0.88
p = 0.0132
d = -0.64
ITPC
ERSP (dB)
Patients
Controls
Frequency (Hz)
Time (s)
t-statistic
dB
Cluster electrodes (n = 22):
Z4, Z5, Z6, Z7, Z9, L4, L5, L6, L7, L8, L9, R4, R5, R6, R7, R9, LL5, LL6, LL7, RR5, RR6, RR8
Cluster electrodes (n = 7):
Z4, Z5, L4, L5, R4, R5, R6
Cluster electrodes (n = 20):
Z4, Z5, Z6, Z7, Z9, L4, L5, L6, L7, L8, L9, R4, R5, R6, R9, LL5, LL6, LL7, RR5, RR6
Cluster electrodes (n = 8):
Z7, L4, L5, L6, L7, L8, LL5, LL6

Figure 3

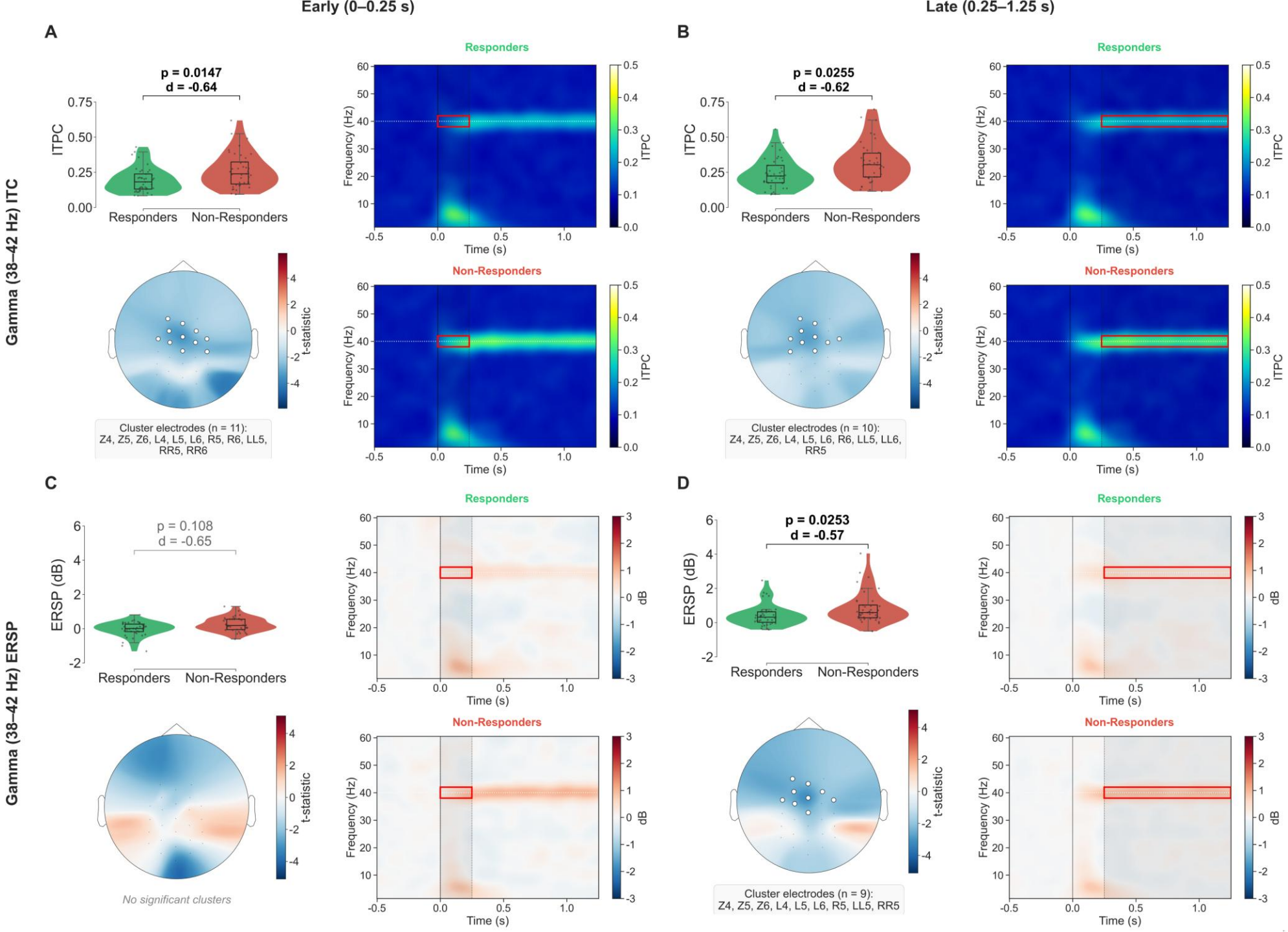

Early (0–0.25 s)
Late (0.25–1.25 s)
A
B
C
D
Gamma (38–42 Hz) ITC
Gamma (38–42 Hz) ERSP
p = 0.0147
d = -0.64
p = 0.0255
d = -0.62
p = 0.108
d = -0.65
p = 0.0253
d = -0.57
ITPC
ERSP (dB)
Responders
Non-Responders
Frequency (Hz)
Time (s)
t-statistic
dB
Cluster electrodes (n = 11): Z4, Z5, Z6, L4, L5, L6, R5, R6, LL5, RR5, RR6
Cluster electrodes (n = 10): Z4, Z5, Z6, L4, L5, L6, R6, LL5, LL6, RR5
No significant clusters
Cluster electrodes (n = 9): Z4, Z5, Z6, L4, L5, L6, R5, LL5, RR5

Figure 4

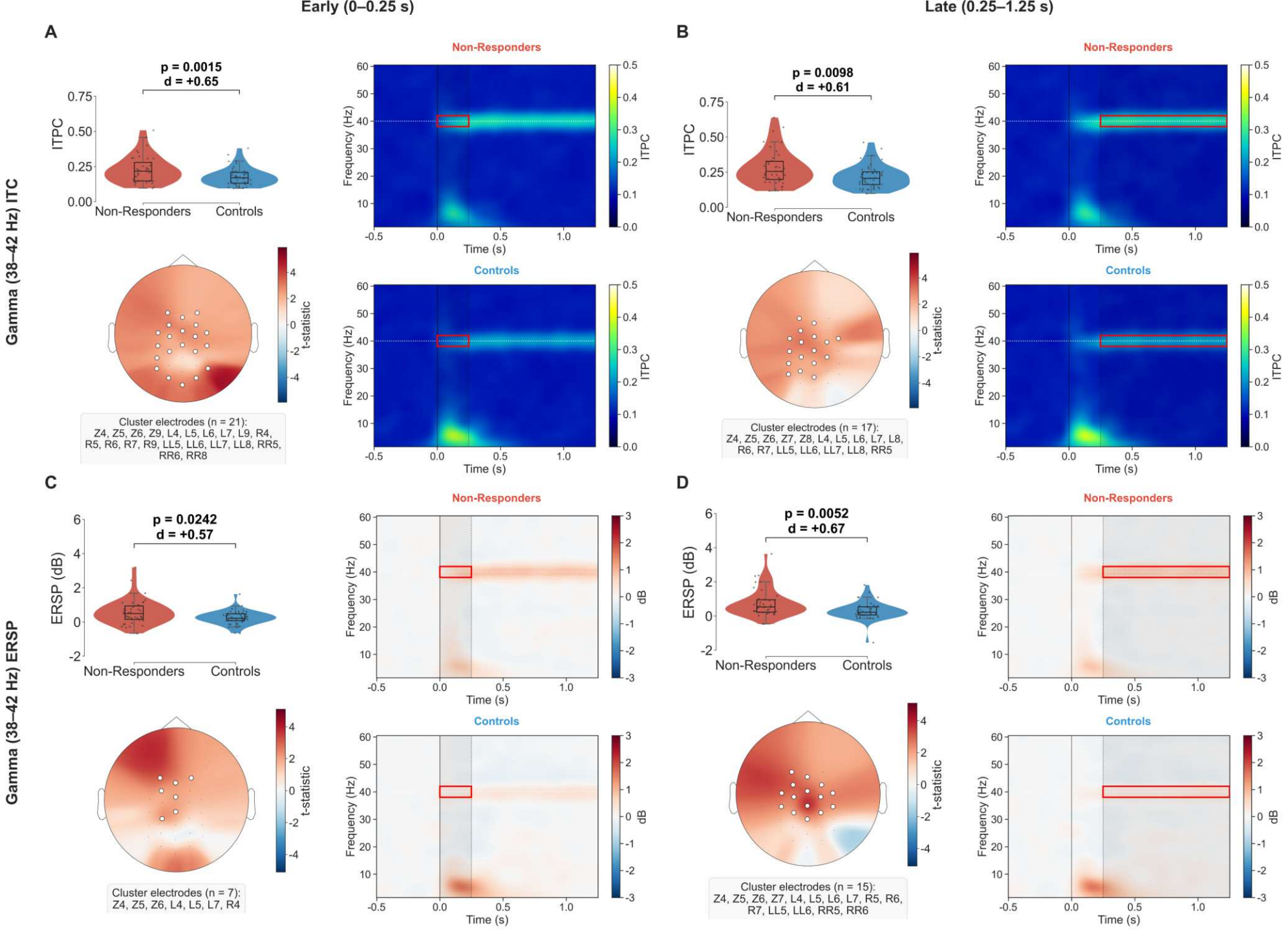

Early (0–0.25 s)
Late (0.25–1.25 s)
A
B
C
D
Gamma (38–42 Hz) ITC
Gamma (38–42 Hz) ERSP
p = 0.0015
d = +0.65
p = 0.0098
d = +0.61
p = 0.0242
d = +0.57
p = 0.0052
d = +0.67
ITPC
ERSP (dB)
Non-Responders
Controls
Frequency (Hz)
Time (s)
t-statistic
dB
Cluster electrodes (n = 21):
Z4, Z5, Z6, Z9, L4, L5, L6, L7, L9, R4, R5, R6, R7, R9, LL5, LL6, LL7, LL8, RR5, RR6, RR8
Cluster electrodes (n = 17):
Z4, Z5, Z6, Z7, Z8, L4, L5, L6, L7, L8, R6, R7, LL5, LL6, LL7, LL8, RR5
Cluster electrodes (n = 7):
Z4, Z5, Z6, L4, L5, L7, R4
Cluster electrodes (n = 15):
Z4, Z5, Z6, Z7, L4, L5, L6, L7, R5, R6, R7, LL5, LL6, RR5, RR6

Figure S1

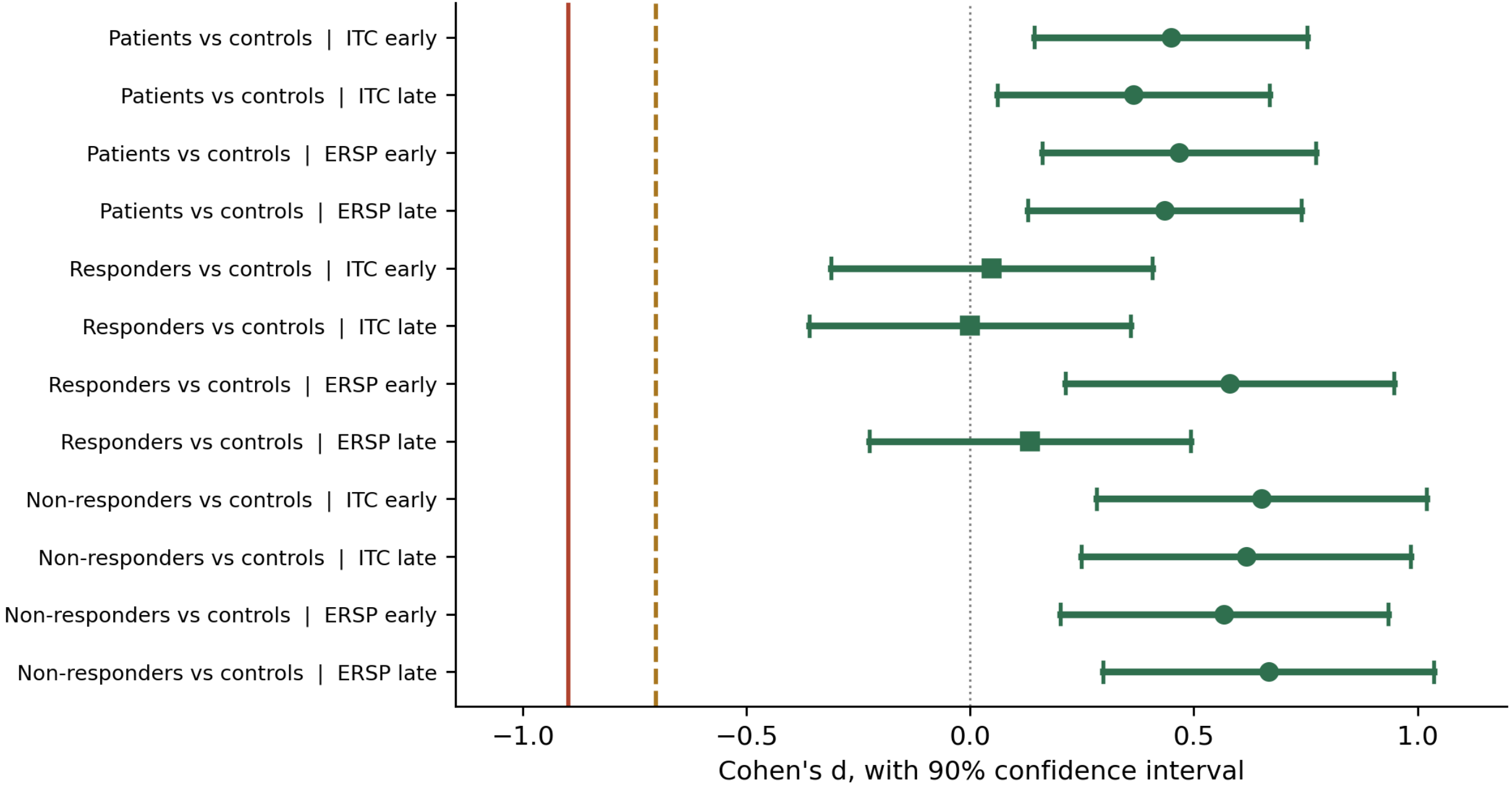

Patients vs controls | ITC early
Patients vs controls | ITC late
Patients vs controls | ERSP early
Patients vs controls | ERSP late
Responders vs controls | ITC early
Responders vs controls | ITC late
Responders vs controls | ERSP early
Responders vs controls | ERSP late
Non-responders vs controls | ITC early
Non-responders vs controls | ITC late
Non-responders vs controls | ERSP early
Non-responders vs controls | ERSP late
−1.0
−0.5
0.0
0.5
1.0
Cohen's d, with 90% confidence interval

Figure S2

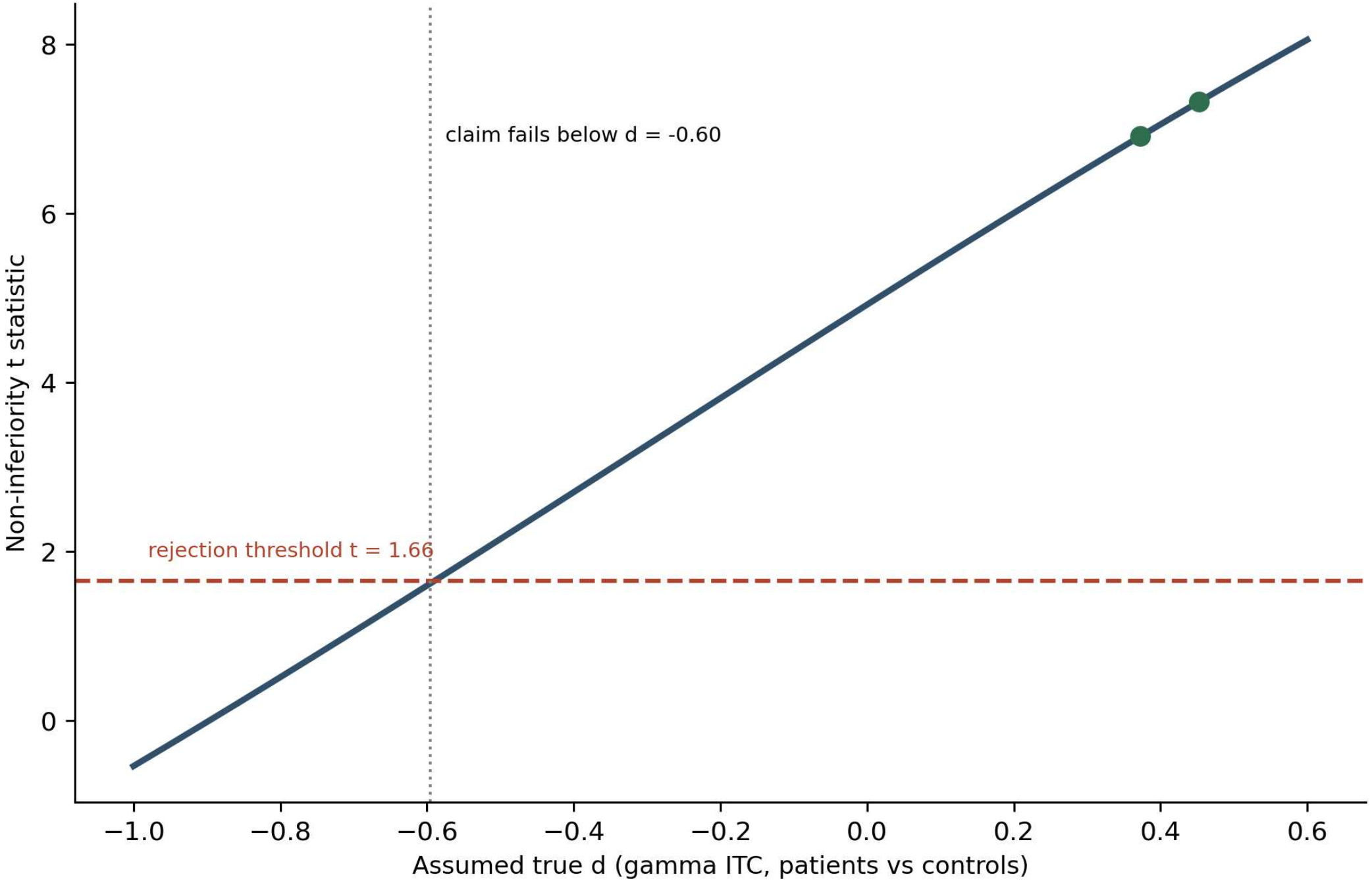
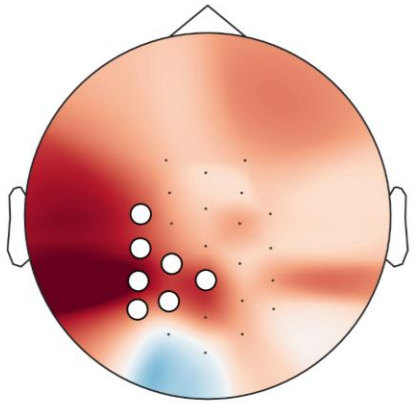
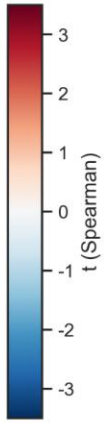

claim fails below d = -0.60
rejection threshold t = 1.66
Non-inferiority t statistic
Assumed true d (gamma ITC, patients vs controls)
8
6
4
2
0
−1.0
−0.8
−0.6
−0.4
−0.2
0.0
0.2
0.4
0.6

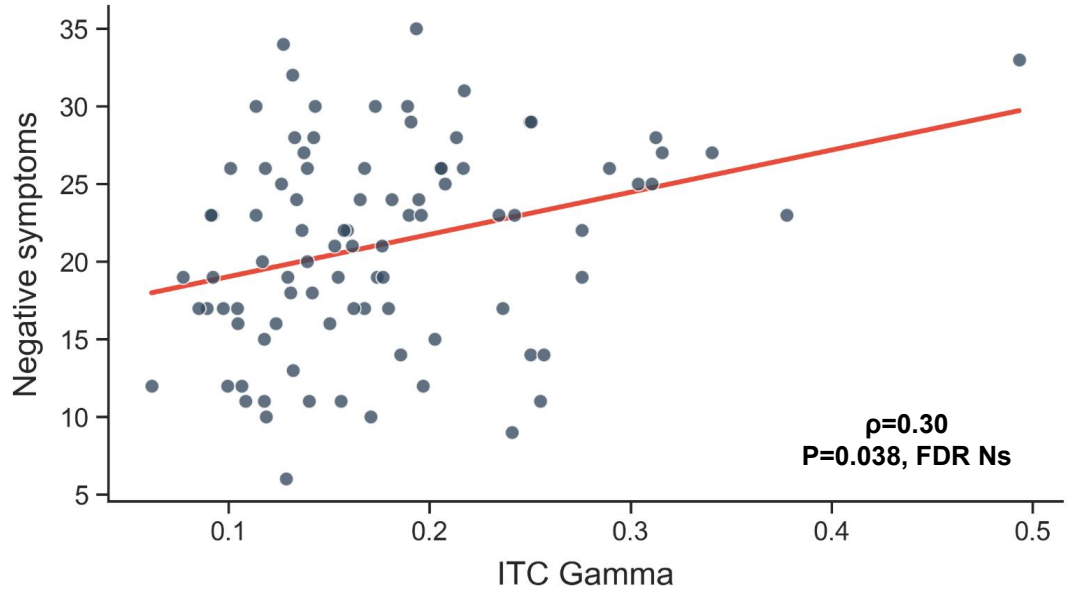
Figure S3

A

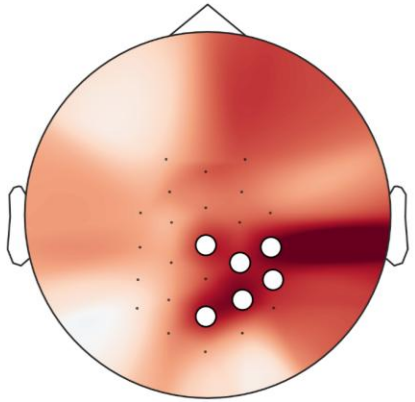


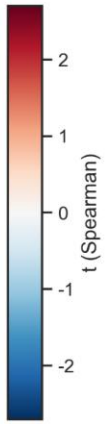


Cluster electrodes (n = 7):
Z7, L7, L8, LL5, LL6, LL7, LL8



B





Cluster electrodes (n = 6):
Z6, Z8, R7, R8, RR6, RR7

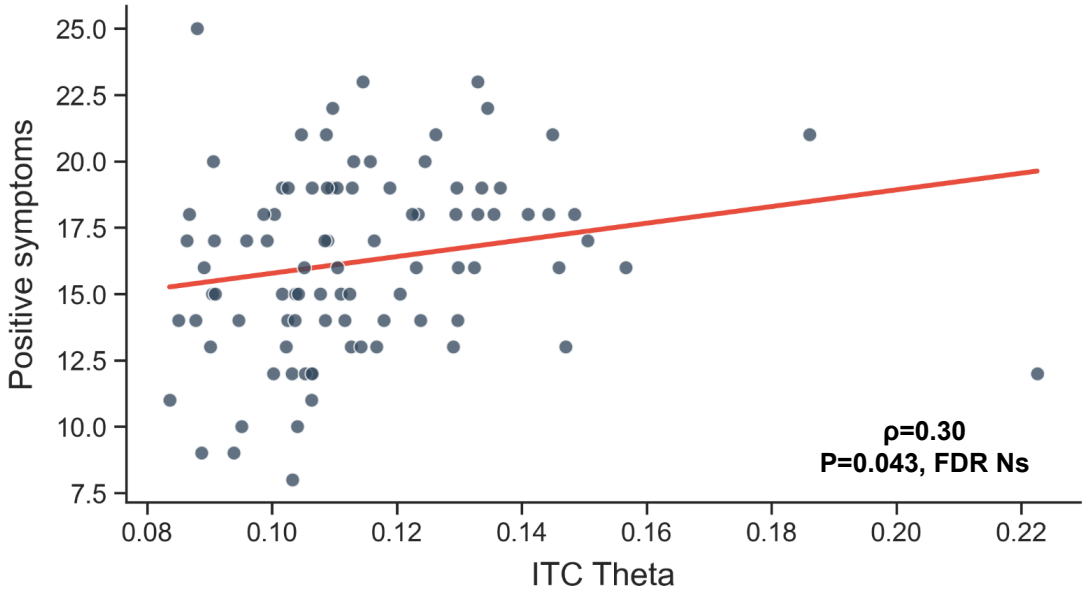
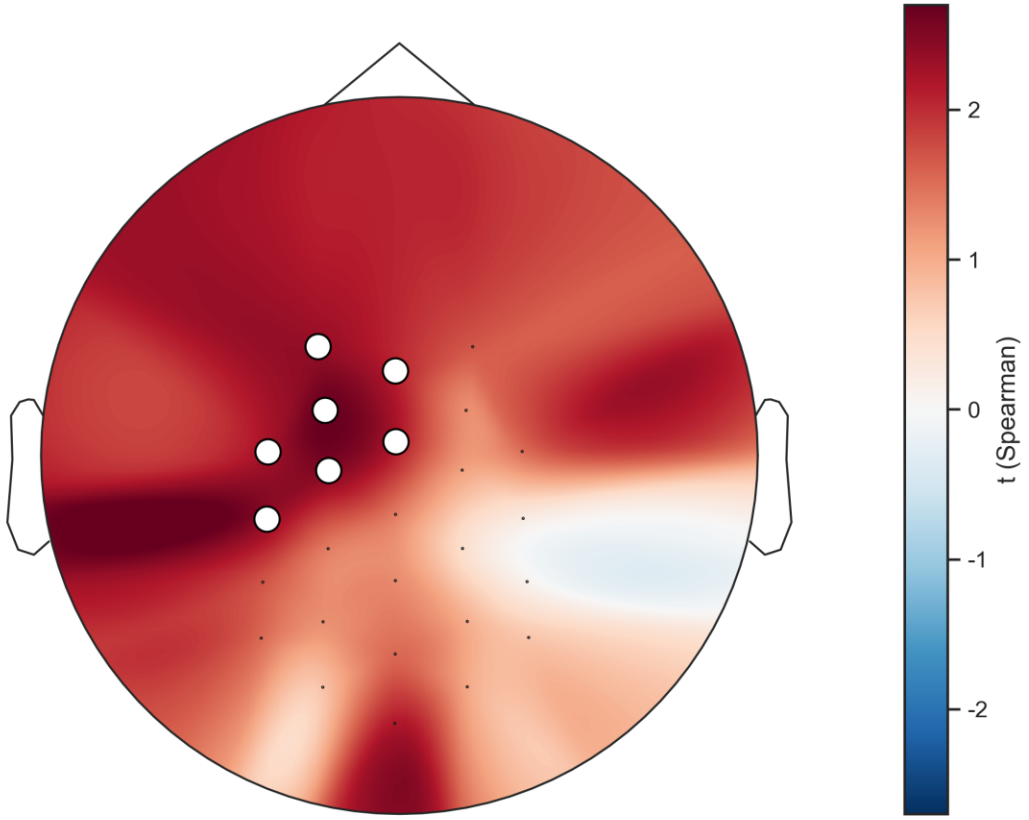


Figure S4



Cluster electrodes (n = 7):
Z4, Z5, L4, L5, L6, LL5, LL6

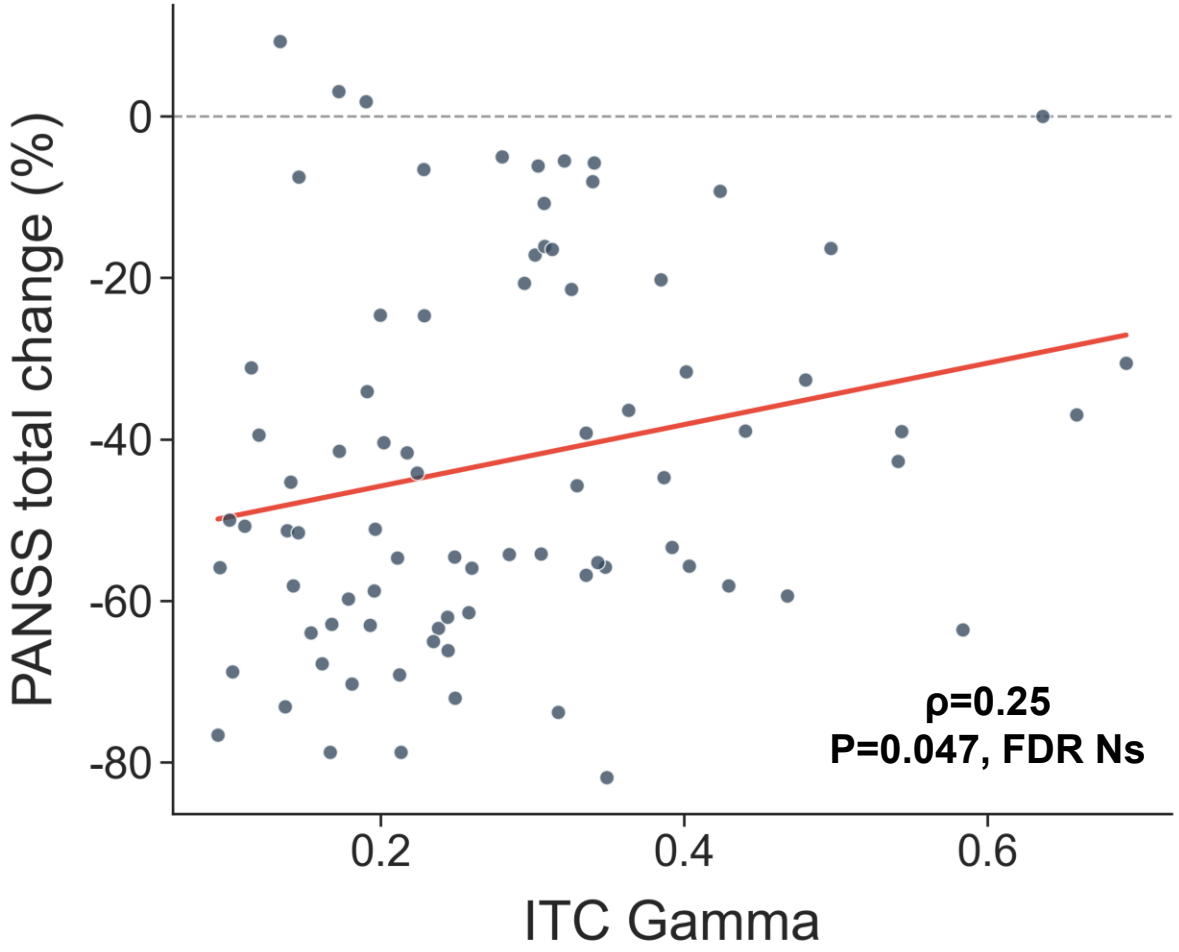


Figure S5

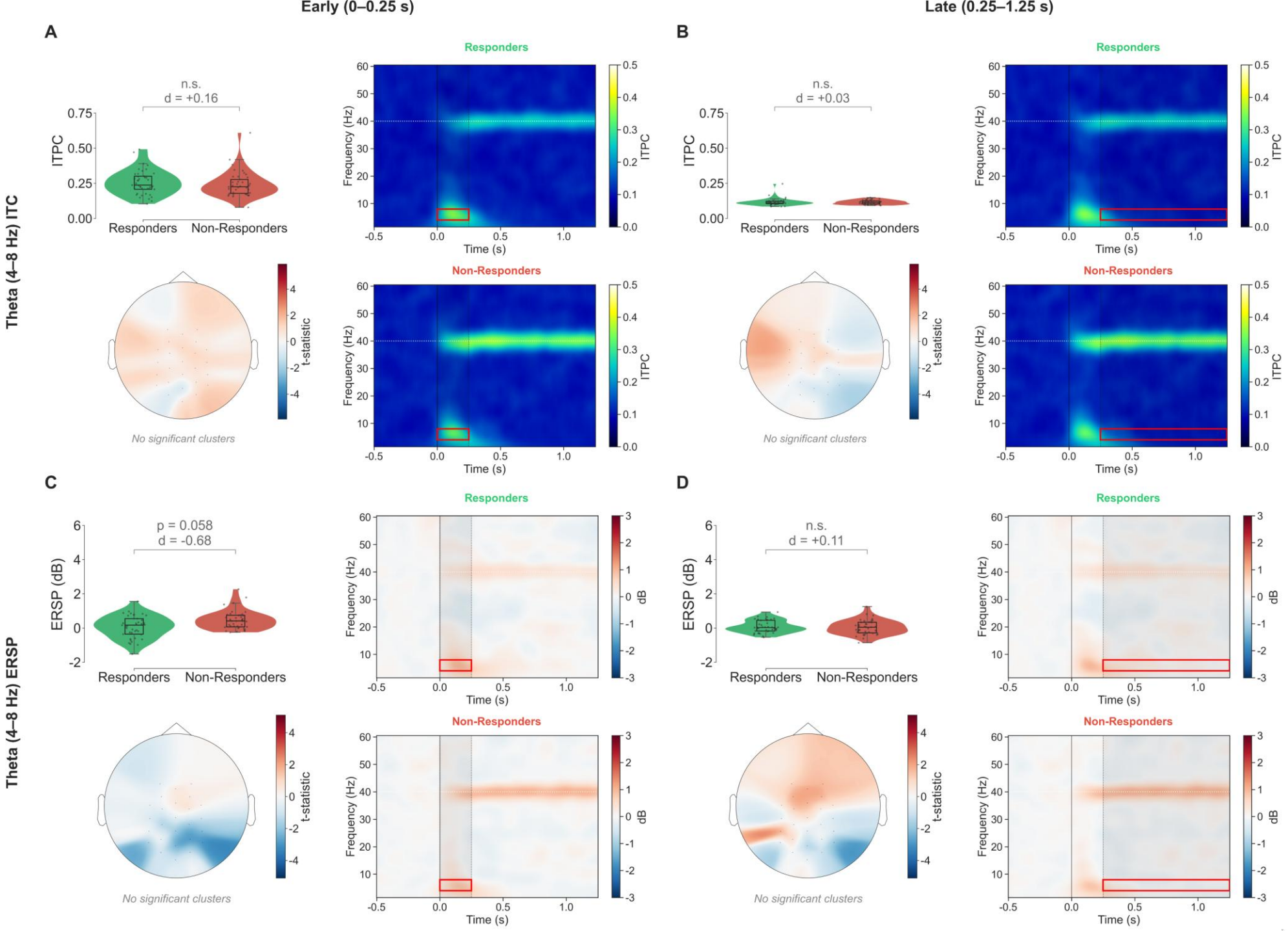

Early (0–0.25 s)
Late (0.25–1.25 s)
A
B
C
D
Theta (4–8 Hz) ITC
Theta (4–8 Hz) ERSP
n.s.
d = +0.16
n.s.
d = +0.03
p = 0.058
d = -0.68
n.s.
d = +0.11
ITPC
ERSP (dB)
Responders
Non-Responders
Frequency (Hz)
Time (s)
t-statistic
dB
No significant clusters

Figure S6

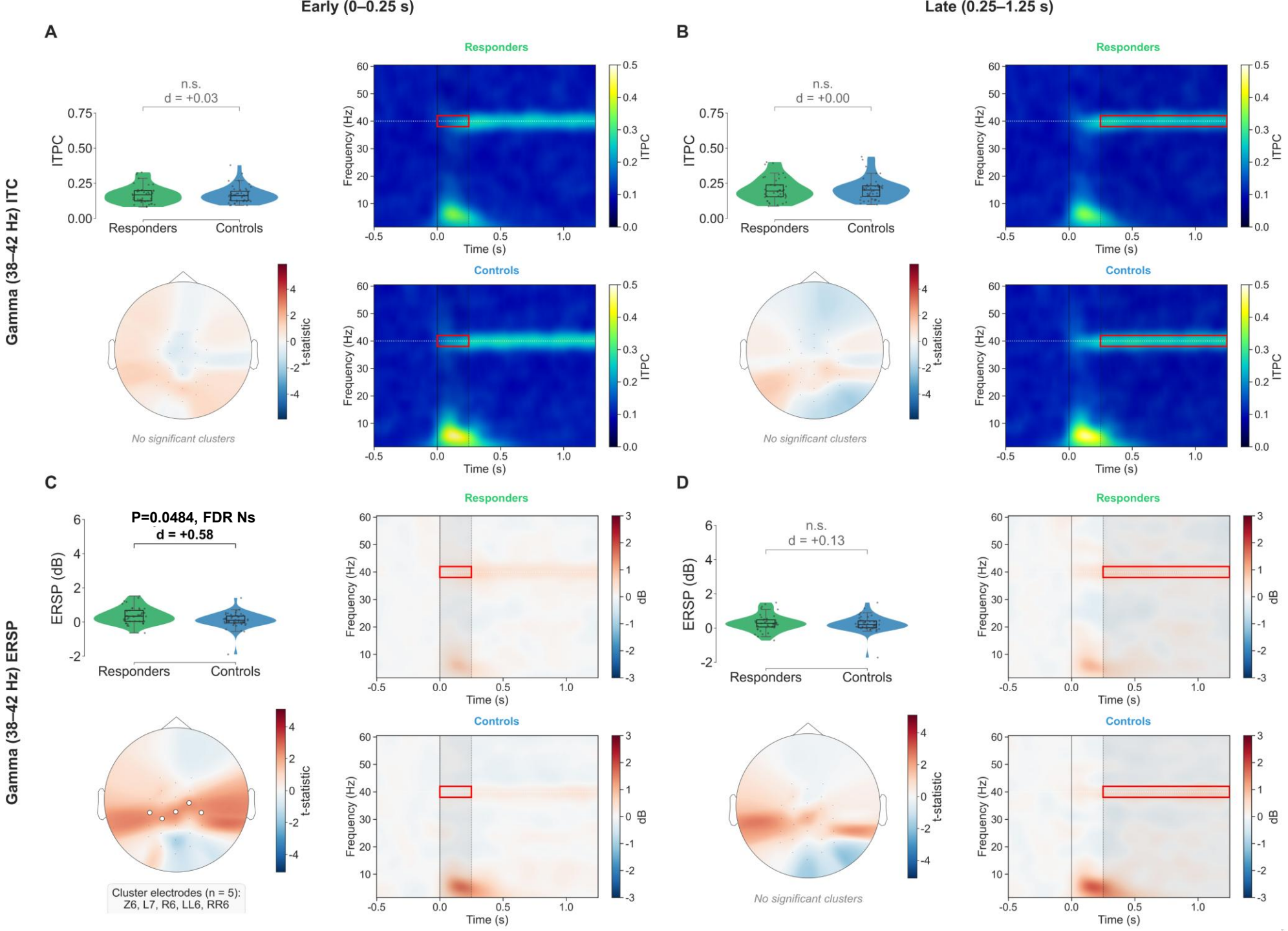

Early (0–0.25 s)
Late (0.25–1.25 s)
A
B
C
D
Gamma (38–42 Hz) ITC
Gamma (38–42 Hz) ERSP
n.s.
d = +0.03
n.s.
d = +0.00
P=0.0484, FDR Ns
d = +0.58
n.s.
d = +0.13
ITPC
ERSP (dB)
Responders
Controls
Frequency (Hz)
Time (s)
t-statistic
dB
No significant clusters
Cluster electrodes (n = 5):
Z6, L7, R6, LL6, RR6

Figure S7

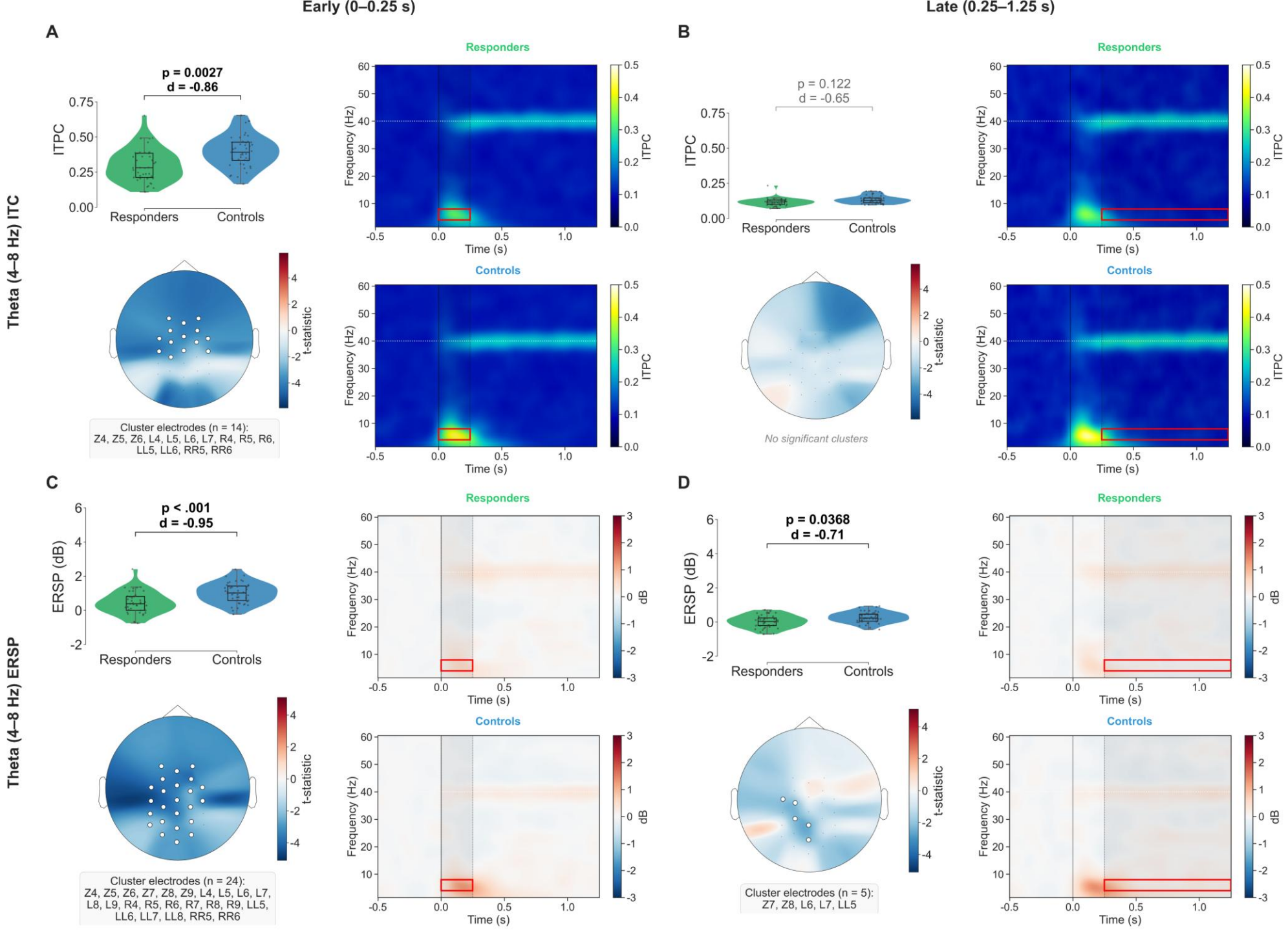

Early (0–0.25 s)
Late (0.25–1.25 s)
A
B
C
D
Theta (4–8 Hz) ITC
Theta (4–8 Hz) ERSP
p = 0.0027
d = -0.86
p = 0.122
d = -0.65
p < .001
d = -0.95
p = 0.0368
d = -0.71
ITPC
ERSP (dB)
Responders
Controls
Frequency (Hz)
Time (s)
t-statistic
dB
No significant clusters
Cluster electrodes (n = 14):
Z4, Z5, Z6, L4, L5, L6, L7, R4, R5, R6, LL5, LL6, RR5, RR6
Cluster electrodes (n = 24):
Z4, Z5, Z6, Z7, Z8, Z9, L4, L5, L6, L7, L8, L9, R4, R5, R6, R7, R8, R9, LL5, LL6, LL7, LL8, RR5, RR6
Cluster electrodes (n = 5):
Z7, Z8, L6, L7, LL5

Figure S8

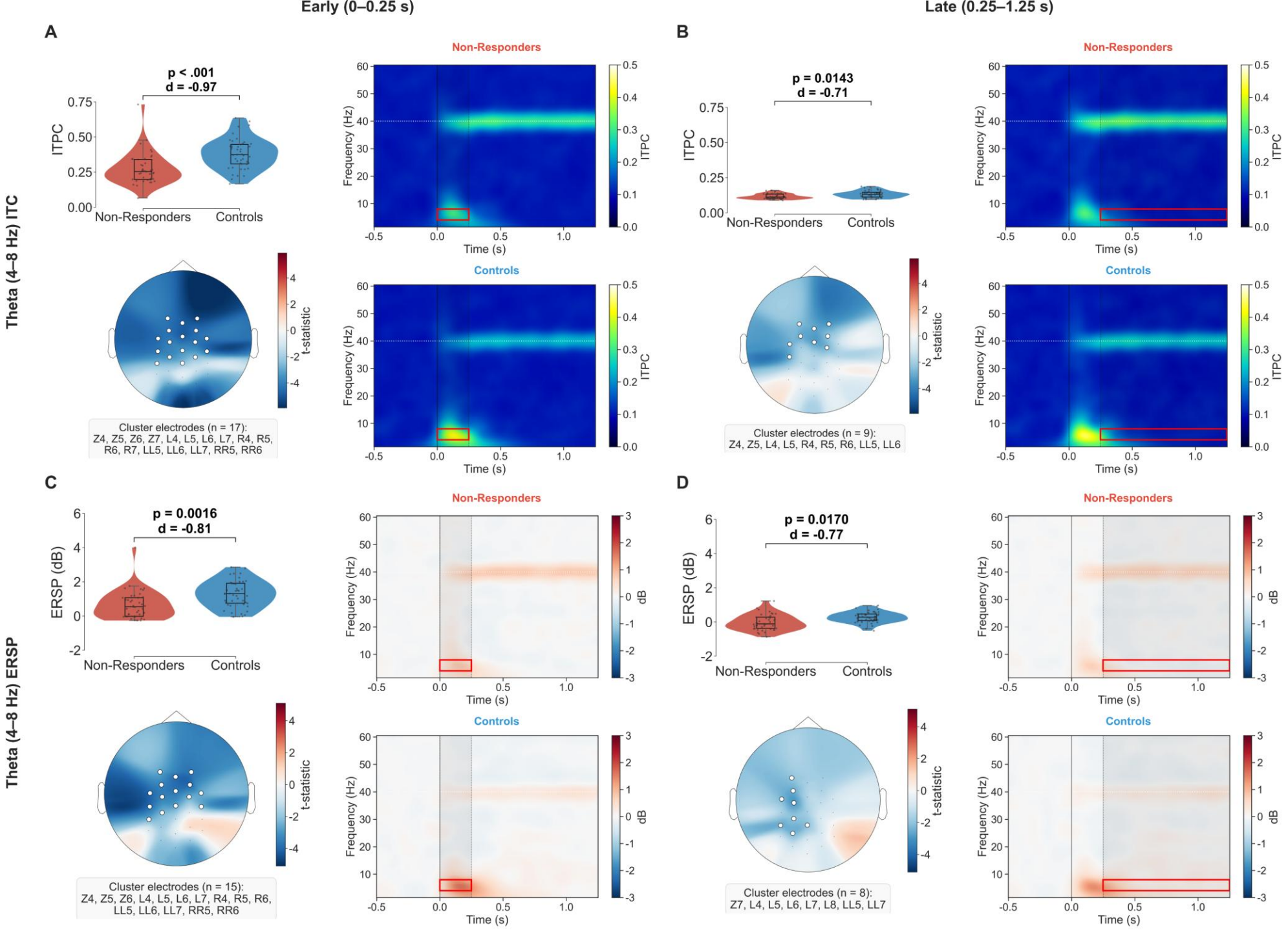

Early (0–0.25 s)
Late (0.25–1.25 s)
A
B
C
D
Theta (4–8 Hz) ITC
Theta (4–8 Hz) ERSP
p < .001
d = -0.97
p = 0.0143
d = -0.71
p = 0.0016
d = -0.81
p = 0.0170
d = -0.77
ITPC
ERSP (dB)
Non-Responders
Controls
Frequency (Hz)
Time (s)
t-statistic
dB
Cluster electrodes (n = 17):
Z4, Z5, Z6, Z7, L4, L5, L6, L7, R4, R5, R6, R7, LL5, LL6, LL7, RR5, RR6
Cluster electrodes (n = 9):
Z4, Z5, L4, L5, R4, R5, R6, LL5, LL6
Cluster electrodes (n = 15):
Z4, Z5, Z6, L4, L5, L6, L7, R4, R5, R6, LL5, LL6, LL7, RR5, RR6
Cluster electrodes (n = 8):
Z7, L4, L5, L6, L7, L8, LL5, LL7

Figure S9

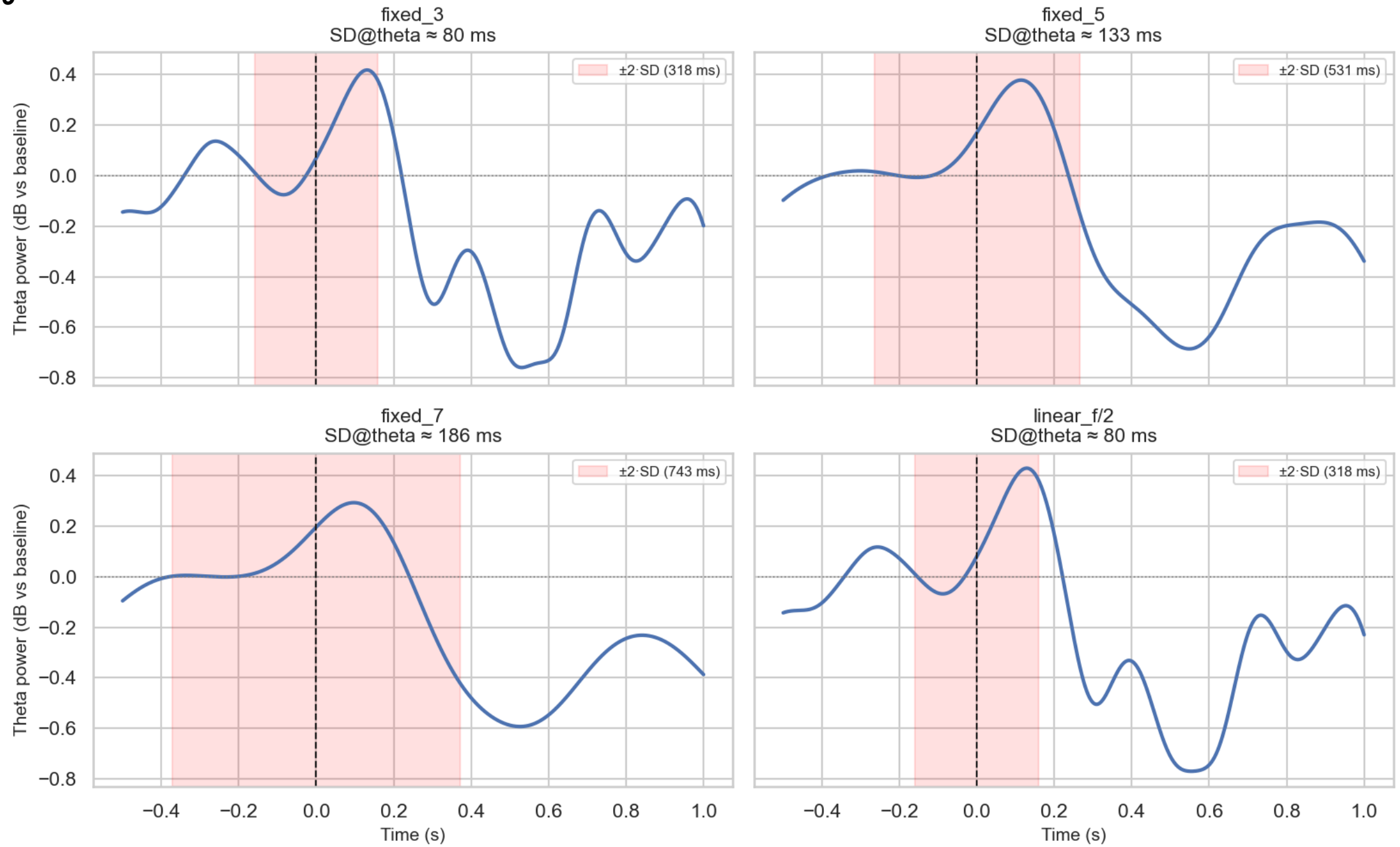

fixed_3
SD@theta ≈ 80 ms
±2·SD (318 ms)
fixed_5
SD@theta ≈ 133 ms
±2·SD (531 ms)
fixed_7
SD@theta ≈ 186 ms
±2·SD (743 ms)
linear_f/2
SD@theta ≈ 80 ms
±2·SD (318 ms)
Theta power (dB vs baseline)
Time (s)
0.4
0.2
0.0
−0.2
−0.4
−0.6
−0.8
−0.4
−0.2
0.0
0.2
0.4
0.6
0.8
1.0

Figure S10

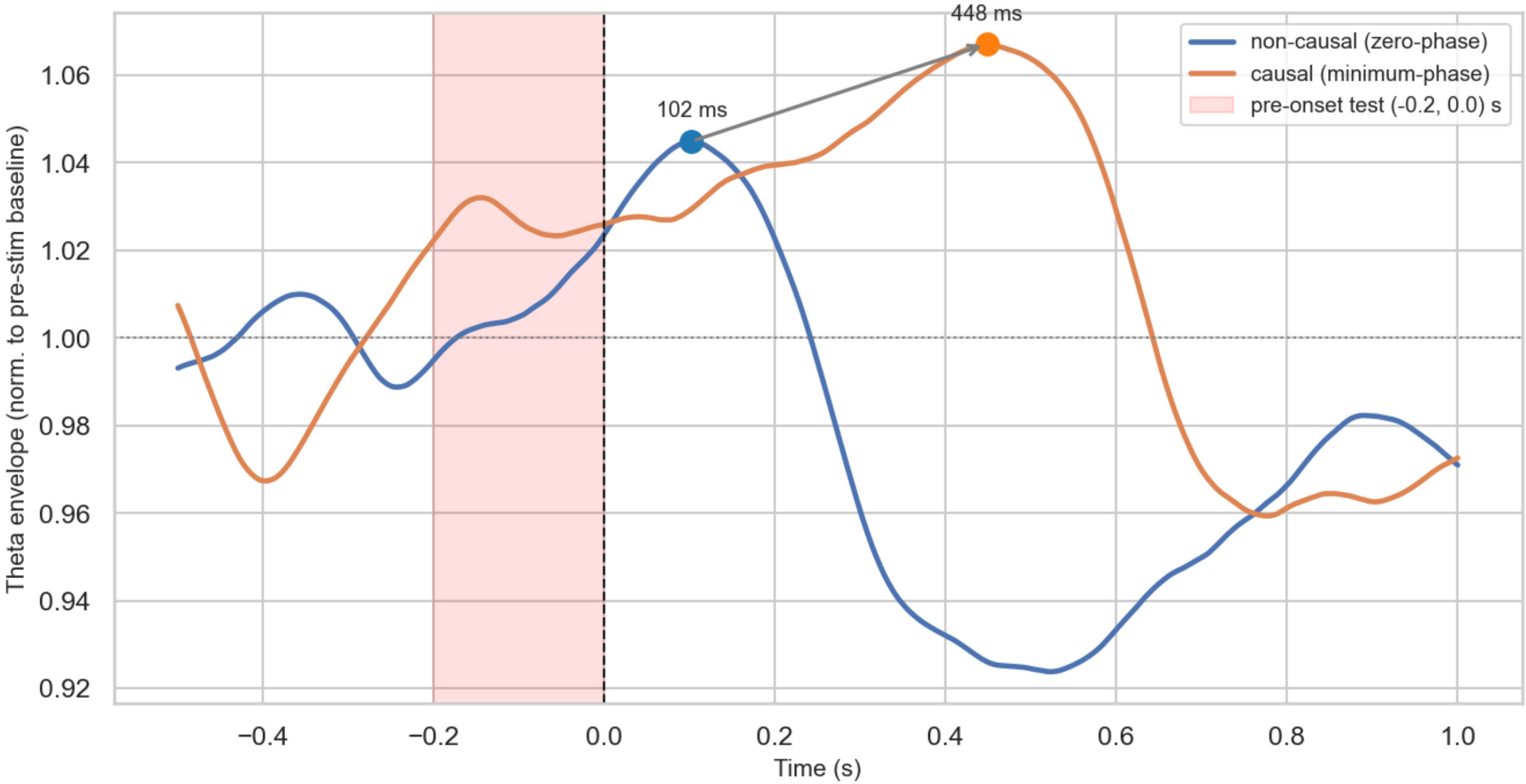
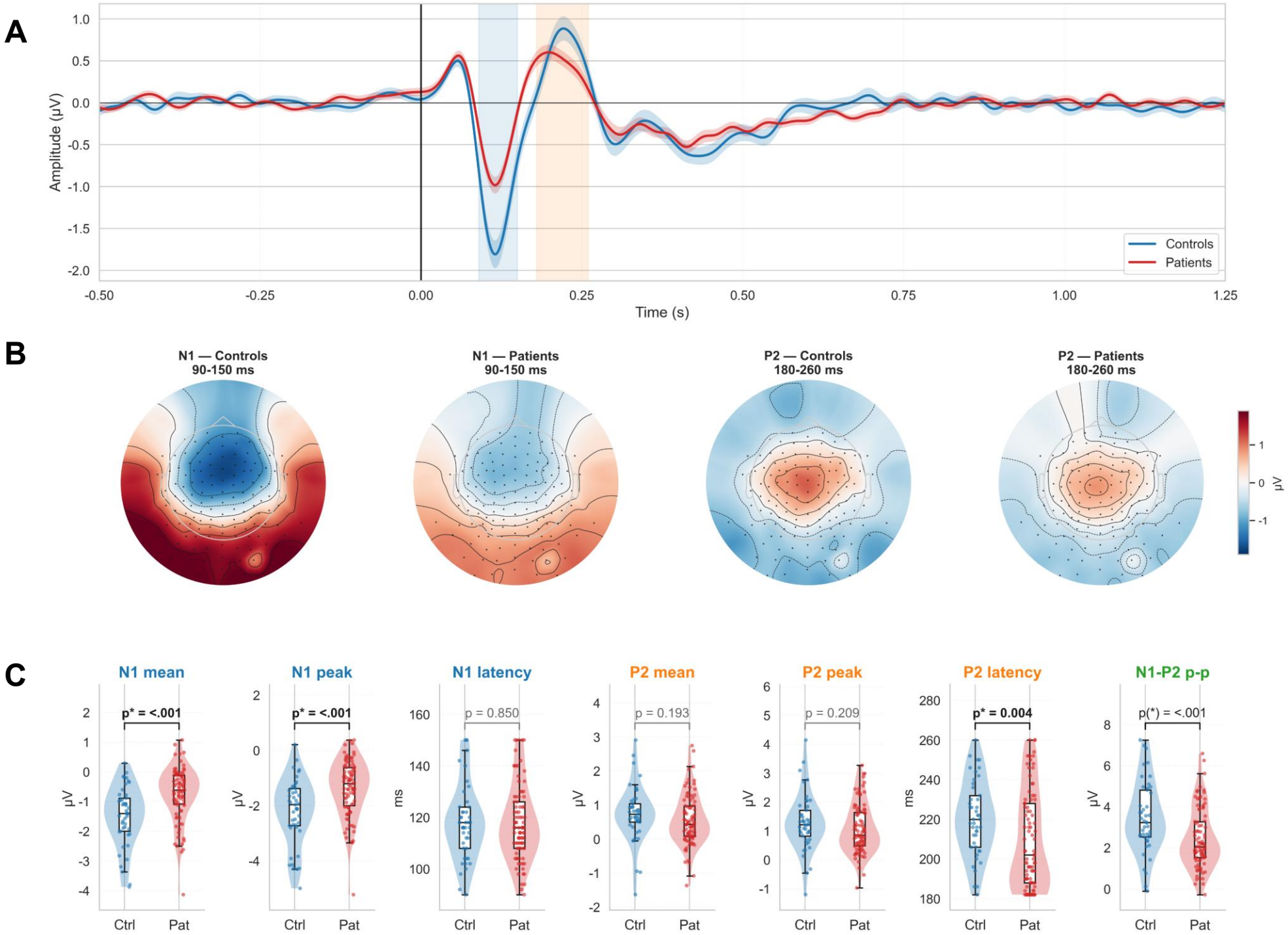

448 ms
102 ms
non-causal (zero-phase)
causal (minimum-phase)
pre-onset test (-0.2, 0.0) s
Theta envelope (norm. to pre-stim baseline)
1.06
1.04
1.02
1.00
0.98
0.96
0.94
0.92
−0.4
−0.2
0.0
0.2
0.4
0.6
0.8
1.0
Time (s)

Figure S11


A
Amplitude (μV)
Time (s)
Controls
Patients
B
N1 — Controls
90-150 ms
N1 — Patients
90-150 ms
P2 — Controls
180-260 ms
P2 — Patients
180-260 ms
μV
C
N1 mean
p* = <.001
N1 peak
p* = <.001
N1 latency
p = 0.850
P2 mean
p = 0.193
P2 peak
p = 0.209
P2 latency
p* = 0.004
N1-P2 p-p
p(*) = <.001
Ctrl
Pat

Supplementary Files

This is a list of supplementary files associated with this preprint. Click to download.

- Tables19.09.2026.docx
- Supplementarymaterials19.09.2026.docx